January 2012

Novel Encapsulation of Oxidizer Applied to Galvanic Cells: Aluminum / H2O2 Galvanic Cell as a Case Study

Marlyn Colon
University of South Florida, mcolon800@gmail.com

Novel Encapsulation of Oxidizer Applied to Galvanic Cells:

Aluminum / H_2O_2 Galvanic Cell as a Case Study

by

Marlyn Colon

A thesis submitted in partial fulfillment
of the requirements for the degree of
Master of Science in Chemical Engineering
Department of Chemical and Biomedical Engineering
College of Engineering
University of South Florida

Co-Major Professor: Norma Alcantar, Ph.D.
Co-Major Professor: Andres M. Cardenas-Valencia, Ph.D.
Ryan Toomey, Ph.D.

Date of Approval:
March 20, 2012

Keywords: Non-Ionic Surfactant, Niosomes, Hydrogen Peroxide Encapsulation,
Poly(N-isopropylacrylamide), Aluminum / Hydrogen Peroxide Galvanic Cell

Dedication

This work is dedicated to my beloved family and friends. Most of all I would like to dedicate this work to my husband for extending his courage, patience, and mental toughness at times when I felt discouraged.

Acknowledgement

I would like to thank my co-major professor Dr. Norma Alcantar for the guidance she has given me on the present work and in life. For the kindness she has shown me throughout my years at USF. I would also like to thank Dr. Andres Cardenas-Valencia, co-major professor. Without his help and mentorship, none of this would have been possible.

- I extend my gratitude to Dr. Ryan Toomey
- A special thank you to my lab mates for continuous support throughout it all- Eva Williams, Audrey Buttice, and Dawn Fox
- I would like to thank Dr. Vinay Gupta and his lab group
- I extend my gratitude to Edward Haller for his assistance in imaging, Electron Microscopy Core Facilities
- SRI, International personnel and facilities
- Funding: Florida Energy Systems Center
- Department of Chemical and Biomedical Engineering, USF

Table of Contents

List of Tables iii

List of Figures iv

Abstract viii

Chapter 1: Introduction 1
1.1 Thesis Outline 1
1.2 Electrochemical Cells 1
1.2.1 Electrochemical Cell Components 3
1.3 Thermodynamics Explanation of Electrochemical Cells 4
1.3.1 Calculation of Cell Electrical Characteristics 7
1.4 Aluminum Anode Electrochemical Cells 9
1.5 Aluminum / Hydrogen Peroxide Galvanic Cell 11
1.6 Research Aims 14
1.7 Proposed Cathode Control System 14

Chapter 2: Cathode Control System 17
2.1 Niosome Composition 17
2.2 Polymer Composition 19

Chapter 3: Experimental Procedures 20
3.1 Niosome Preparation 20
3.2 NIPAAm Preparation 22
3.3 Cell Potential Experiments versus Time 23

Chapter 4: Results and Discussion 27
4.1 Niosome Size Characterization 27
4.1.1 Niosome Size Distribution Study 27
4.1.2 Dynamic Behavior of Niosome's Diameter for Long Term Stability 34
4.1.3 Niosome Size Distribution Before and After Extrusion 36
4.2 Investigation of Proposed System Compared to Traditional Al / H_2O_2 System 39
4.2.1 Premise of Investigation 39

4.2.2 Results from Investigation of Proposed System Utilizing Al Purity of 99.99% 40
4.2.3 Comparison of Cell Characteristics between SPAN 40 and SPAN 60 Composed Niosomes 46
4.2.4 Comparison of Different Aluminum Purities on Proposed System ...54
4.2.5 Investigation of Proposed System with Alternating the Degree of Cross-linking for Poly(N-isopropylacrylamide) Polymer 62

Chapter 5: Conclusion and Future Work 70
5.1 Summary of Findings....70
5.2 Future Work Recommendations 74
5.2.1 Continuing Niosome Size Characterization 74
5.2.2 Future Cell Potential Experiments 74
5.3 Final Remarks 75

References.... 76

List of Tables

Table 1: Equations for Electrical Performance Characteristics for Electrochemical Cells [8] 8

Table 2: Electrochemical Cells Incorporating the Use of Aluminum [13, 14] 10

Table 3: Amount of Energetic Output per Amount of Al Consumed for Niosomes in Suspension (Without Polymer) 53

Table 4: Amount of Energetic Output per Amount of Al Consumed for Novel Proposed System 53

Table 5: Average Energetic Output for Al Purities: 99.998% & 99.99% 58

Table 6: Percent Decrease in Power Output Value Compared to Control (0.119 W) 66

Table 7: Percent Change in Al Consumption Value Compared to Control (0.181 g Al): Red Value Indicate an Increase in Al Consumption 67

Table 8: Average Energetic Output Obtained / Average Value of Al Consumed; Values Utilizing Al Purity 99.99% with Varying Amounts of BisAAm (Polymer Cross-Linker) 69

List of Figures

Figure 1: Basic Components of an Electrochemical Cell 4

Figure 2: Example of Cell Potential Curve for Niosome Experimental Run Utilizing 99.99% Al Purity (Average of Five Experiments Conducted) 8

Figure 3: Example of Instantaneous Power Curve for Niosome Experimental Run Utilizing 99.99% Al Purity (Average of Five Experiments Conducted); Area Underneath Curve is Equal to the Cell's Energetic Output 9

Figure 4: Illustration of Proposed System 16

Figure 5: A.) Sorbitan Monopalmitate (SPAN 40, 14 Carbon Chain), B.) Sorbitan MonoStearate (SPAN 60, 15 Carbon Chain) [28].....17

Figure 6: Cholesterol Structure [38] 18

Figure 7: DCP Structure [39]..... 18

Figure 8: NIPAAm Chemical Structure [40]..... 19

Figure 9: BisAAm Chemical Structure [41] 19

Figure 10: Thin Film Hydration Method; Figure A: Hydration of Thin Film, Figure B: Formation of Niosomes Once Thin Film is no Longer Visible 21

Figure 11: Electrodes and Dielectric Material 23

Figure 12: A.) Figure of Experimental Setup at Cell Position 6; B.) Figure of Experimental Setup at Cell Position 4; C.) Top View of Cell Stack with Numbered Cells 25

Figure 13: Polymer before Mixing Niosome Solution, Clear Separation..... 25

Figure 14: Polymer after Mixing Niosome Solution 26

Figure 15: Size Distribution for SPAN 60 Niosomes: Batch 1; Measurement Taken on the Day Niosomes were Prepared 29

Figure 16: Size Distribution for SPAN 60 Niosomes: Batch 2; Measurement Taken on the Day Niosomes were Prepared 30

Figure 17: Size Distribution for SPAN 60 Niosomes: Batch 3; Measurement Taken on the Day Niosomes were Prepared 31

Figure 18: TEM Image of Sample from Batch 3 (SPAN 60 Niosomes) at 7.1KX Magnification: Image Displays Niosomes on the Lower End of the Size Distribution Curve Shown in Figure 17 32

Figure 19: TEM Image of Sample from Batch 3 (SPAN 60 Niosomes) at 7.1KX Magnification: Image Displays Niosomes on the Upper End of the Size Distribution Curve Shown in Figure 17 33

Figure 20: Niosomes' Hydrodynamic Diameter versus Time for Batch 1, 2, & 3 35

Figure 21: Size Distribution for Niosomes Before and After Extrusion; Batch 1 37

Figure 22: Size Distribution for Niosomes Before and After Extrusion; Batch 2 38

Figure 23: Average Cell Overall Power Output Utilizing Al Purity 99.99% 42

Figure 24: Average Cell Op. Times Utilizing Al Purity 99.99%..... 43

Figure 25: Average Al Consumption Values Utilizing Al Purity of 99.99% 44

Figure 26: Energy per Al Consumed in Grams Utilizing Al Purity of 99.99% (Numbers in Red Indicated Percent Change Compared to Control) 45

Figure 27: Size Distribution Curve for SPAN 40 Niosomes (Three Different Batches) Utilized in SPAN 40 vs. 60 Niosome Experiments.....48

Figure 28: Size Distribution Curve for SPAN 60 Niosomes (Three Different Batches) Utilized in SPAN 40 vs. 60 Niosome Experiments.....49
Figure 29: Average Power Output Utilizing Al Purity 99.99%, SPAN 40 vs. SPAN 60 Niosomes (Numbers in Red Indicated Percent Difference between Values) 50
Figure 30: Average Cell Op. Time Utilizing Al Purity 99.99%, SPAN 40 vs. SPAN 60 Niosomes (Numbers in Red Indicated Percent Difference between Values) 51
Figure 31: Average Al Consumption Utilizing Al Purity 99.99%, SPAN 40 vs. SPAN 60 Niosomes (Numbers in Red Indicated Percent Difference between Values) 52
Figure 32: Average Overall Cell Power Output Values for Al Purities: 99.998%, 99.99%, & 99.90% (Numbers in Red Indicated Percent Change Compared to Control).....56
Figure 33: Average Aluminum Consumption Values for Al Purities: 99.998%, 99.99%, & 99.90% (Numbers in Red Indicated Percent Change Compared to Control).....57
Figure 34: Average Cell Operational Time Values for Al Purities: 99.998%, 99.99%, & 99.90% (Numbers in Red Indicated Percent Change Compared to Control).....57
Figure 35: Energy (KJ) per Consumption of Aluminum (gram of Al) for Al Purities: 99.998%, 99.99%, & 99.90%.....60

Figure 36: Energy (KJ) per Consumption of Aluminum (Dollar of Al) for Al Purities: 99.998%, 99.99%, & 99.90%.....60

Figure 37: Energy (KJ) per Consumption of Aluminum (Dollar of Al) for Al Purities: 99.998% & 99.99% 61

Figure 38: Average Cell Overall Power Output Values Utilizing Al Purity 99.99% with Varying Amounts of BisAAm (Polymer Cross-Linker).....64

Figure 39: Average Cell Op. Time Values Utilizing Al Purity 99.99% with Varying Amounts of BisAAm (Polymer Cross-Linker) 65

Figure 40: Al Consumption Average Values Utilizing Al Purity 99.99% with Varying Amounts of BisAAm (Polymer Cross-Linker) 68

Abstract

The work presented in this thesis aims to address the obstacles that side reactions create in aluminum / H_2O_2 galvanic cells by proposing to control the cathodic reactant, H_2O_2, via encapsulation. Encapsulation of the cathodic reactant is achieved utilizing a non-ionic surfactant vesicle (i.e. niosome). Once encapsulated, a second control element over the cathodic reactant is provided. The use of a polymer will be implemented to achieve stability and render further control over the encapsulated H_2O_2 solution. Implementation of the proposed novel cathodic control system in aluminum / H_2O_2 galvanic cells aims to minimize aluminum consumption and increase cell efficiency. Cell performance is evaluated by several electrical characteristics which include and are not limited to cell overall power output, cell operational time, and energy production per consumption of the aluminum anode. Results indicate an average energetic output value of 0.57 KJ +/- 0.09 KJ versus 0.542 KJ +/- 0.05 KJ without the implementation of the proposed cathodic control system. In addition, a decrease of 15% in average aluminum consumption value was achieved with the use of the proposed system.

Chapter 1: Introduction

1.1 Thesis Outline

This thesis presents a novel control system that will assist in the development of the selected aluminum / H_2O_2 electrochemical cell. Chapter one introduces the use of electrochemical cells implemented in a range of applications and further explains a cell's components. In addition, a detailed explanation of thermodynamics and cell electrical characteristics are provided. Due to the fact that an aluminum anode electrochemical cell was chosen as the case study, background information on aluminum anode systems is included in chapter one. Chapter two provides preliminary information on the proposed system. Chapter three conveys details on the methodology and procedures followed throughout the experimentation process. Chapter four is a discussion of results acquired for this body of work. Chapter five summarizes the results and provides recommendations for future work on this project

1.2 Electrochemical Cells

In an electrochemical cell, chemical energy is converted directly into electric energy. This conversion of energy is due to oxidation and reduction reactions that occur within the cell [1]. Electrochemical cells that have spontaneous electrode reduction/oxidation reactions occurring are termed galvanic cells [2]. Electrochemical power sources are portable, flexible in size, and silent [3]. Currently electrochemical cells are utilized in a wide range of applications from powering portable electronic devices to

electric vehicles [1]. In addition, electrochemical cells are utilized in the extraction process of metals from aqueous solution. In air, metal ore is roasted to produce a metal oxide. Sequentially, it is dissolved in an acidified aqueous solution contained in the galvanic cell. Appling an electrical current to the cell will allow the metal to be electrochemically deposited at the cathode [2]. Metals such as Pb, Zn, Ni, Co, Cd, Cr, Sn, and Mn are electrochemically extracted.

In addition, electrochemical cells are utilized in batteries. Batteries are comprised of more than one electrochemical cell connected in series, parallel, or a combination of both. Batteries have the ability to store electrical energy supplied from an external source and power portable devices [1]. The worldwide market for batteries value exceeds 100 billion dollars with the majority resulting from lead-acid batteries [3].

Other electrochemical cells of interest are fuel cells. Fuel cells are similar to batteries in the way they operate. The difference between a battery and a fuel cell is where the reactants are contained. For fuel cells, there is an external fuel source supplying the electrochemical cell as for batteries, it is contain within the cell [1]. Fuel cells have been under extensive research over the years and incorporated in a range of applications from powering spacecrafts to unmanned underwater vehicles[4, 5]. In particular, the hydrogen / oxygen fuel cell has been implemented into powering fuel cell vehicles [6]. A single hydrogen / oxygen fuel cell produces approximately 1 V under open circuit conditions and are connected in series, to form a stack, to obtain higher voltage values [7].

1.2.1 Electrochemical Cell Components

There are three basic components to an electrochemical cell, as shown in Figure 1. The first component is a negative electrode commonly known as the anode. Oxidation occurs at the surface of the anode generating electrons. The electrons flow through an external electrical circuit and reach the second component of the cell, the positive electrode commonly known as the cathode. At the cathode, consumption of the electrons occurs via a reduction reaction. Balancing the transfer of electrons, occurring in the external electrical circuit, are negative and positive ions present in an electrolyte medium. Positive ions flow towards the cathode and the negative ions flow towards the anode. This ionic conductor is the third component in an electrochemical cell known as the electrolyte [1]. Electrolytes that are not electrically conductive and have good ionic conductivity are ideal to use in cells [1].

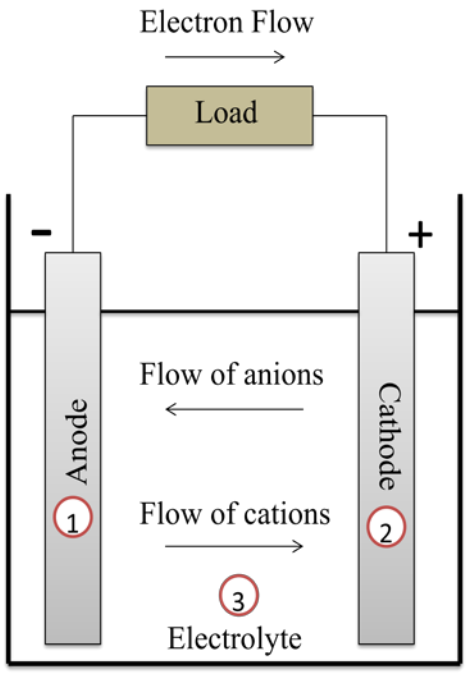

Figure 1: Basic Components of an Electrochemical Cell

1.3 Thermodynamics Explanation of Electrochemical Cells

If the net reaction in an electrochemical cell is reversed by applying a current flow in the opposite direction, the cell is said to be reversible. The cell reaches an equilibrium state when no current is being drawn. The measured difference in potential across the terminals of a reversible cell at an equilibrium state is termed the electromotive force (emf) of the cell and also known as the open circuit voltage [3]. As chemical reactions arise in the electrochemical cell, there is a decrease in free energy that enables the cell to deliver electric energy to an external circuit [1]. This change in free energy is equaled to the thermodynamically available work. Utilizing the electrical energy produced by the electrochemical cell divided by the thermodynamically available work results in the cell's

energy efficiency. The emf of a cell may be related to the change in free energy shown in Equation 1.

$$\Delta G^o = -nFE^o \quad (1)$$

Where F = Faraday's Constant, equaled to 96,500 Coulomb

n = number of electrons involved in stoichiometric reaction

E^o = Standard Electromotive force/ Standard Cell Potential

Utilizing standard oxidation and reduction potentials for the anodic and cathodic electrode reactions, the standard potential for an electrochemical cell may be obtained (Equation 2 [8]). These oxidation and reduction potentials are thermodynamically predicated values affiliated with a reference half reaction. The accepted half reaction reference is the standard hydrogen electrode where hydrogen gas at one bar is utilized to saturate an electrode comprised of a noble metal [3].

$$Anode\ (oxidation\ potential) + Cathode\ (reduction\ potential) = Standard\ Cell\ Potential \quad (2)$$

If conditions are not in the standard state, the Nernst equation may be used for any given cell (Equation 3).

$$E = E^o - \frac{RT}{nF} \ln \left[\frac{a^{vp} \ldots\ldots}{a^{vr} \ldots\ldots} \right] \quad (3)$$

Where F = Faraday's Constant, equaled to 96,500 Coulomb

n = number of electrons involved in stoichiometric reaction

E^o = Standard Electromotive force / Standard Cell Potential

a= activity coefficient of individual components / species

vp= stoichiometric coefficient for product species

vr= stoichiometric coefficient for reactant species

Thermodynamically predicated cell potentials are always higher then cells under a load. The deviation from predicated values is termed the overpotential [8]. The difference in voltage values are due to losses within the cell from internal resistance [3]. During the presences of a current, internal resistance in the bulk of the electrode and electrolyte phases causes a decrease in cell potential [8]. The loss in voltage due to internal resistance (IR) is commonly known as ohmic loss / IR drop [3].

Concentration and activation overpotentials are two factors that also contribute to a cell's overpotential value [8]. Concentration overpotential is associated with the mass transfer limitations of reactants and products at the interface between the electrode and electrolyte. In other words, concentration gradients at the electrode surface inhibit current generation [3]. Activation overpotential incorporates limitations due to rate determining

steps in the electrode reaction. These rate determining steps dedicate how the reaction will proceed kinetically [8]. The contribution due to activation overpotential usually is not significant in a cell's overpotential [8].

1.3.1 Calculation of Cell Electrical Characteristics

Once the cell is activated, voltage values versus cell operational time (defined as the time for a cell to reach a voltage value of 0.6 Volts) are closely monitored and are the basis for the parameters implemented in characterizing the cell's performance. Figure 2 and 3 are examples of cell potential versus time curves and instantaneous power versus time curves. Figures 2 and 3 are an average of five experimental runs. Standard deviation values were obtained and displayed in both figures.

The performance of the aluminum anode galvanic cell is evaluated by taking into account the obtained instantaneous power, which is dependent on the electrical load subject upon the cell [9]. Integrating instantaneous power with respect to time defines the discrete amount of work produced, equation shown in Table 1. By knowing the amount of provided work, overall power output values can be calculated (equation displayed in Table 1 [9]).

Table 1: Equations for Electrical Performance Characteristics for Electrochemical Cells [8]

Instantaneous Power at time { P(t) }	$P(t) = \frac{V(t)^2}{R}$
Provide Work (W)	$W = \int_{t=0}^{t=top} P(t)\, dt$
Cell Overall Power Output (P)	$P = \frac{W}{top}$

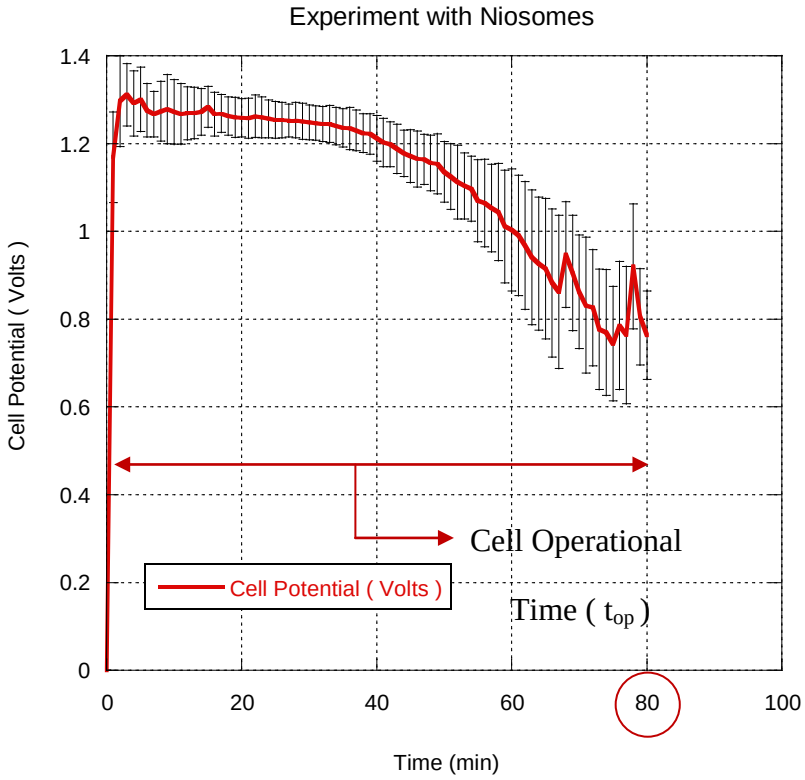

Figure 2: Example of Cell Potential Curve for Niosome Experimental Run Utilizing 99.99% Al Purity (Average of Five Experiments Conducted)

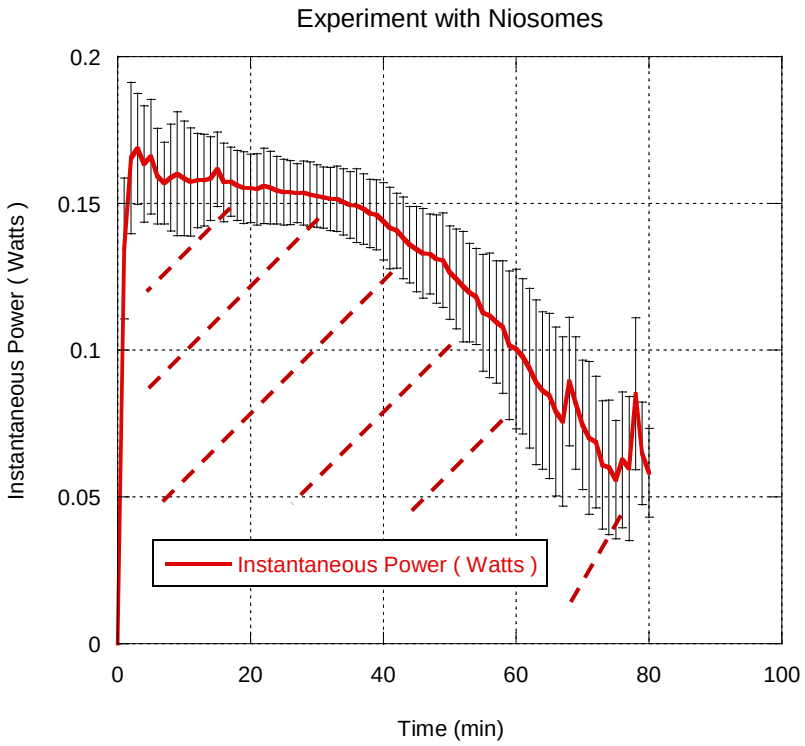

Figure 3: Example of Instantaneous Power Curve for Niosome Experimental Run Utilizing 99.99% Al Purity (Average of Five Experiments Conducted); Area Underneath Curve is Equal to the Cell's Energetic Output

1.4 Aluminum Anode Electrochemical Cells

Low density materials with high theoretical oxidation potentials are ideal for the manufacturing of the negative electrode/anode in an electrochemical cell. Other qualities such as stability, conductance, and cost contribute in the selection process [1]. Focus on the use of magnesium and aluminum as anodes have been noted in literature [10]. Aluminum, in particular, is attractive as a negative electrode material due to its oxidation potential of +1.7V and low density [11, 12]. In addition, aluminum's reported theoretical energy density is among the highest in electrochemical cells with a value of 24.7 KJ / gram [12].

The usage of Aluminum for electrode material has been around since 1850s and was first introduced as an negative electrode material in the Buff cell in 1857 [13]. Reporting's of an aluminum zinc alloy anode for chlorine depolarized batteries emerged in 1948 and by 1950 considerable efforts occurred in the development of aluminum anode power systems [13]. Since then several systems have emerged implementing the use of aluminum as the anode material, refer to Table 2.

Table 2: Electrochemical Cells Incorporating the Use of Aluminum [13, 14]

Al Anode Electrochemical Cells
Al / MnO_2
Al / AgO
Al / S
Al / FeCN
Al / NiOOH
Al / $C_3N_3Cl_3O_3$
Al / Na_2O_2
Al / H_2O_2

1.5 Aluminum / Hydrogen Peroxide Galvanic Cell

Zaromb in 1960 pioneered initial research on aluminum / hydrogen peroxide galvanic cells [11]. This system implements the use of hydrogen peroxide as the cathodic reactant present in an alkaline media [13]. The initial presence of hydroxide ions is required to initiate the electrochemical reaction for the aluminum / hydrogen peroxide galvanic cell, refer to Equation 4 [5, 9, 13]. The electrochemical reaction for the aluminum hydrogen peroxide system has a theoretical standard potential (E^o) of 3.2 Volts [12]. In order for the electrochemical reaction to establish its self, the cathode reaction, shown as Equation 5, must occur [9, 15].

Electrochemical Reaction: $2Al_{(s)} + 3H_2O_{2(aq)} + 2OH^{-1}_{(aq)} \rightarrow 2Al(OH)^{-1}_{4(aq)}$ $E^o = 2.3V$ (4)

Cathode Reaction: $H_2O_{2(aq)} + OH^{-1}_{(aq)} + 2e \rightarrow 3OH^{-1}_{(aq)}$ $E^o = 0.87\ V$ (5)

As the electrochemical reaction proceeds, it has been reported in literature that the concentration of aluminate, $2Al(OH)^{-1}_4$, increases and the concentration of the hydroxide ion decreases [5]. This decrease in concentration of hydroxide ions is interrupted by the precipitation of aluminum hydroxide, $2Al(OH)_3$, shown by Equation 6 [16].

$$Al(OH)^{-1}_4 \rightarrow Al(OH)_3 + OH^- \quad (6)$$

Side reactions do arise and in return interfere with the electrochemical reaction and ultimately reduces energy production. These side reactions are parasitic in nature consuming both anode and cathode materials. There are three main side reactions of concern.

- The corrosion of aluminum [5, 11, 17]:

$$2Al_{(s)} + 3H_2O \rightarrow 2Al(OH)_{3(s)} + 3H_{2(g)} \quad (7)$$

- The direct reaction of aluminum with hydrogen peroxide [5, 9]:

$$2Al_{(s)} + 3H_2O_{2(aq)} \rightarrow 2Al(OH)_{3(s)} \quad (8)$$

- The decomposition of hydrogen peroxide[15, 17, 18]:

$$2H_2O_{2(aq)} \rightarrow O_{2(g)} + 2H_2O_{(l)} \quad (9)$$

In the corrosion of aluminum, the anode material is consumed inadequately and hydrogen gas is created. The corrosion of aluminum reaction is detrimental to the cell's efficiency and the creation of hydrogen gas forms bubbles that hinder viable electrode surface area. The direct reaction of aluminum with hydrogen peroxide forms precipitates of aluminum hydroxide. A thin coating on the anode is developed as a result of the direct reaction. Another parasitic reaction is the decomposition of hydrogen peroxide where cathodic reactant is exhausted. Hydrogen peroxide reacts in the presence of contaminates and innately decomposes [11].

In an attempt to control parasitic reactions from occurring, the use of small amounts of other materials infused into the aluminum anode has been investigated [19]. Previously evaluated aluminum alloys incorporate the use of Ga, In, Sn, Zn, Ma, Ca, Pb, and Mn [20]. Altering cell structure has been noted in literature to improve cell efficiency

by adjusting anode to cathode surface area [9]. The use of a cationic surfactant, cetyl trimethyl ammonium bromide (CTAB), in combination with lupine seed extract has been investigated to inhibit the aluminum corrosion reaction that occurs [21]. To prevent the direct reaction of H_2O_2 with aluminum, an ion diffusion membrane has been used in previous studies to obstruct the passage of H_2O_2 molecules [22]. In cell designs where an ion diffusion membrane is absent, additives have been explored, such as gallium oxide and sodium plumbate, that assist in the removal of the formed thin coating on the anode that results from the direct reaction [19]. In addition, the use of a Pd- Ir catalyst and metallic silver catalyst (deposited onto a Ni foam substrate) have both been explored to improve upon the reduction of H_2O_2 (positively affecting the electrochemical efficiency) [17, 23]. Furthermore, attempts to improve cell efficiency have focused on the use of slow dissolving solid oxidizers [24]. Conjointly, the solid oxidizers were encapsulated utilizing gelatin and acrylamide polymers [25]. Adequate encapsulation of liquid oxidizers for use in galvanic cells may be challenging.

1.6 Research Aims

The work presented in this thesis aims to address the obstacle that side reactions create by proposing to control the cathodic reactant, H_2O_2, via encapsulation. Once encapsulated, the use of a polymer will be implemented to further control the release of H_2O_2. Implementation of the proposed novel control system is hypothesized to minimize aluminum consumption, reduce side reactions and increase cell efficiency. Research aims are shown below.

- Increase Power Generation- Through consuming material adequately by reducing parasitic reactions via novel reagent control system.
- Reduce Aluminum Consumption- Results in material conservation and prolongs the utilization of the electrochemical cell.

1.7 Proposed Cathode Control System

The first component of the proposed system is a non-ionic surfactant vesicle known as a niosome. These vesicles are formed through the self-assembly of non-ionic amphiphilic surfactants, in an aqueous media, into spherical bilayer structures [26]. Factors that contribute to vesicle formation include the temperature of the medium, surfactant monomer structure, and concentration [27]. The structure of a niosomes is composed of a hydrophobic shell and a hydrophilic core [28]. Niosomes differ from other types of vesicles, such as liposomes or polysomes, in their basic unit of assembly. Liposomes are composed of natural, charged amphiphilic lipids and polysomes are built with copolymers of amphiphilic characteristics [28]. The preferred use of niosomes over liposomes is attributed to its chemical stability, lower cost of chemicals, and a substantial amount of surfactant options [29]. Initial research on non-ionic surfactants vesicles was

conducted in the seventies by the cosmetic industry [26]. Since then, there utilization has expanded into the biomedical industry, where they have been investigated as drug carriers [26-28].

The niosomes will be utilized, in this body of work, to encapsulate aqueous hydrogen peroxide solutions (oxidizer) providing an initial control over the release rate. To minimize instability due to osmotic pressure caused by differences in solute concentrations, the niosomes are suspended into the same hydrogen peroxide solution used in the encapsulation process [27]. The suspended niosome solution is exposed to a second control element proposed in the present work.

The second component of the proposed system is a three dimensional polymer network chemically crossed linked into a gel-like substance [30]. Implementing the use of a polymer allows for a second control over the release of hydrogen peroxide. Figure 4 illustrates the proposed system presented in this body of work. Diffusion of encapsulated hydrogen peroxide and hydrogen peroxide molecules into the polymer network will occur once the polymer is in contact with the suspended niosome solution ensuring a second control over the cathodic reactant.

The selected polymer was synthesized from N-isopropylacrylamide (NiPAAm) monomers by free radical polymerization. Poly(N-isopropylacrylamide) is a thermo-responsive hydrogel that exhibits a phase transition at temperatures higher than 32 degrees Celsius [31]. The hydrogel will transition from a swollen to a shriveled state once temperatures are above 32 degrees Celsius [32]. At these higher temperatures, the expulsion of solvent that occurs is due to hydrophobic interactions [30]. Thermo-

responsive hydrogels are an attractive class of material and are currently being studied in applications of separation systems [33, 34], chemo-mechanical values [35], and drug delivery systems [36].

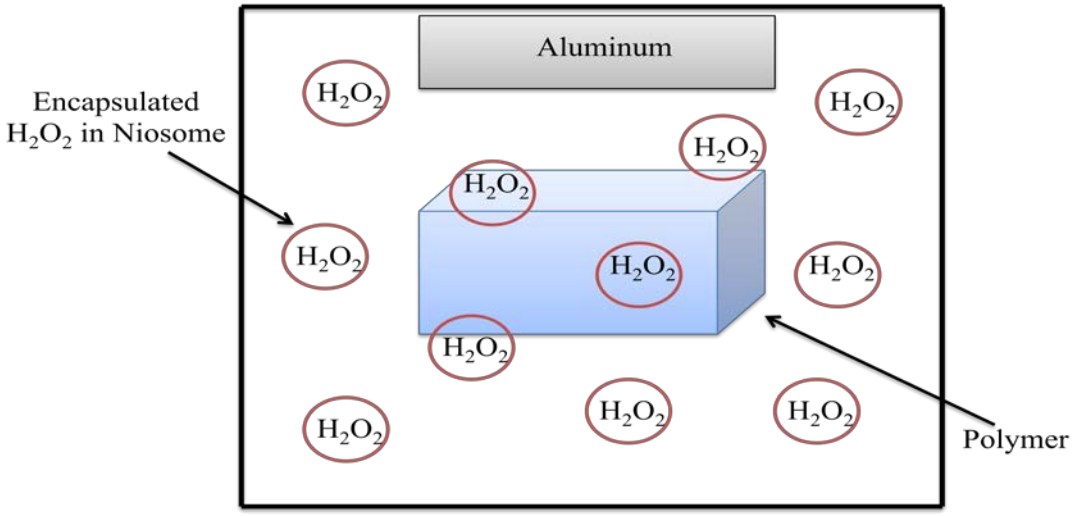

Figure 4: Illustration of Proposed System

Chapter 2: Cathode Control System

2.1 Niosome Composition

The niosomes utilized for this body of work are composed of a non-ionic surfactant, cholesterol, and dicetyl phosphate free acid. The non-ionic surfactant chosen are two sorbitan esters. The first is Sorbitan Monopalmitate (SPAN 40) with a molecular weight of $402\ \frac{g}{mole}$ and a molecular formula of $C_{22}H_{42}O_6$. The second sorbitan ester is Sorbitan Monostearate (SPAN 60) with a molecular weight of $430.63\frac{g}{mole}$ and a molecular formula of $C_{24}H_{46}O_6$. Both SPAN 40 and 60 were acquired from Sigma-Aldrich and their catalog numbers are 388920-250G and S7010-250G respectively. It has been previously noted in literature that entrapment efficiencies are highest with the implementation of either SPAN 40 or SPAN 60 surfactant for niosome formation [37].

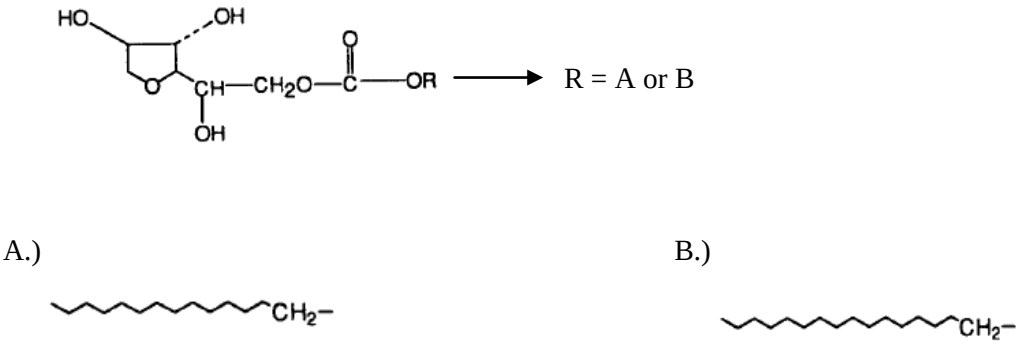

Figure 5: A.) Sorbitan Monopalmitate (SPAN 40, 14 Carbon Chain), B.) Sorbitan MonoStearate (SPAN 60, 15 Carbon Chain) [28]

The second component is cholesterol having a molecular weight of 386.66 $\frac{g}{mole}$ and a molecular formula of $C_{27}H_{46}O$. Figure 6 shows the chemical structure of cholesterol. Incorporating cholesterol in niosome formation has been cited to contribute to the niosome's stability and to provide certain rigidity in the assembly process [28]. The cholesterol purchased was ovine wool > 98% grade from Avanti Polar Lipids, catalog number 700000p (5 g).

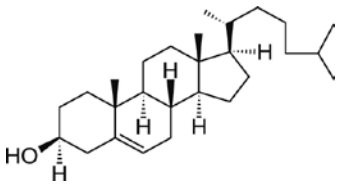

Figure 6: Cholesterol Structure [38]

The third component is dicetyl phosphate free acid (DCP) having a molecular weight of $546.85\frac{g}{mole}$ and molecular formula of $C_{32}H_{67}O_4P$. Figure 7 shows its' chemical structure. This compound was purchased from MP Biomedicals LLC, catalog number 101546 (1 g). The utilization of dicetyl phosphate helps protect against flocculation of vesicles in suspension [27].

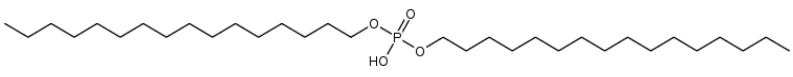

Figure 7: DCP Structure [39]

2.2 Polymer Composition

N-isopropylacrylamide (NIPAAm) functional monomer has a molecular formula of $C_6H_{11}NO$ and a molecular weight of $113\ \frac{g}{mole}$(Figure 8). NIPAAm was purchased from Sigma-Aldrich, catalog number 415324 (97%). The solvent utilized to dissolve the monomer is deionized (D.I.) water. The chemical cross-linker selected is N,N'-methylenebisacrylamide (BisAAm). The chemical cross-linker has a molecular formula of $C_7H_{10}N_2O_2$ and molecular weight of $154.17\frac{g}{mole}$ (Figure 9). BisAAm was purchased from Sigma-Aldrich, catalog number 146072 (99%). The initiator chosen is ammonium persulfate (APS). The initiator has a molecular formula of $(NH_4)_2S_2O_8$ and a molecular weight of $228.20\frac{g}{mole}$. APS was purchased from Sigma-Aldrich, catalog number 248614 ($\geq 98.0\%$). The activator used is N,N,N',N'-tetramethylethylenediamine (TEMED). The activator has a chemical formula of $C_6H_{16}N_2$ and a molecular weight of $116.21\frac{g}{mole}$. TEMED was purchased from TEKNOVA, catalog number T0761 (ultra-pure grade).

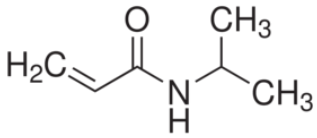

Figure 8: NIPAAm Chemical Structure [40]

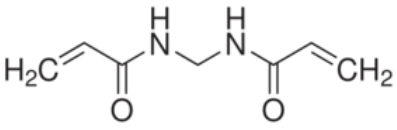

Figure 9: BisAAm Chemical Structure [41]

Chapter 3: Experimental Procedures

3.1 Niosome Preparation

The niosomes were prepared in a 1:1:0.95 molar ratio of SPAN 60: cholesterol: DCP. The mass amount of SPAN 60 used for niosome formation is 0.098g (0.092g of SPAN 40 was used for the preparation of SPAN 40 niosomes). As for DCP and cholesterol, 0.013g and 0.88g were utilized respectively. The three chemicals were dissolved into 3 mL of chloroform and placed into a 100 mL round bottom flask. The solution was rotated in a water bath having a temperature of 60 degrees Celsius. This temperature was selected due to it being above the phase transition temperature of SPAN 60 (about 50 degrees Celsius [37]). Once all the chloroform was evaporated, a thin film was formed (approximately 20 minutes). The thin film was purged with nitrogen for approximately 5 minutes and covered with parafilm®. The covered flask remained clapped upside down to further dry for 8-24 hours.

The film was hydrated with 4 mL 30% wt solution of hydrogen peroxide creating the self-assembly formation of niosomes as shown in Figure 10. Stock solutions of 30% wt hydrogen peroxide were obtained by further diluting 50% wt hydrogen peroxide solution purchased from Fisher, catalog number H341-500, with D.I. water. Stock solutions of 30% wt hydrogen peroxide were remade after a period of 5-7 days. The niosome solution was sonicated for 15 minutes. Once sonicated, the niosome solution was extruded through a polycarbonate membrane, purchased from Avanti Polar Lipids

catalog number 610004 pore size of 0.08 micrometer. The niosome solution was suspended into 30% wt hydrogen peroxide solution. A volume ratio of 0.25 (niosome solution formed after hydration / hydrogen peroxide solution) was utilized.

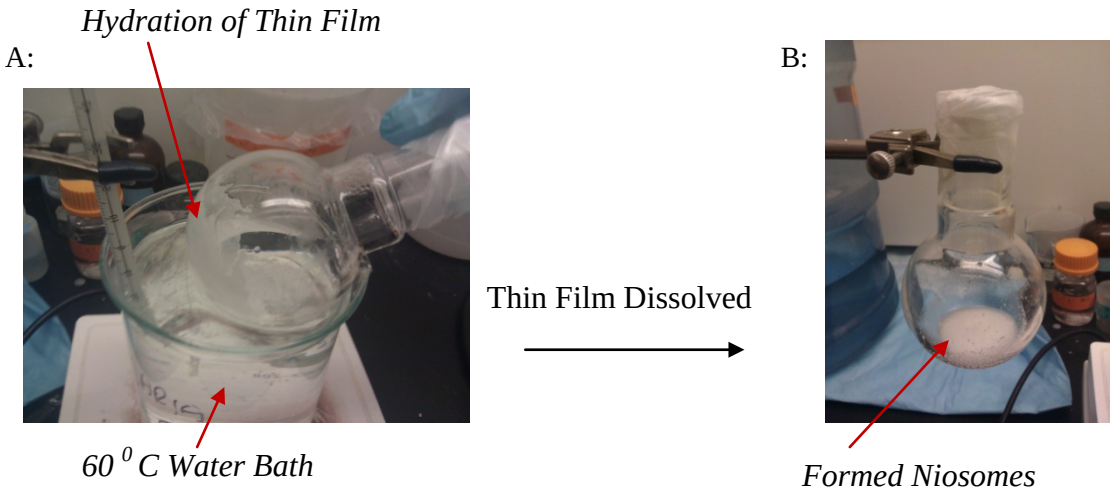

Figure 10: Thin Film Hydration Method; Figure A: Hydration of Thin Film, Figure B: Formation of Niosomes Once Thin Film is no Longer Visible

3.2 NIPAAm Preparation

The selected polymer was synthesized from N-isopropylacrylamide (NIPAAm) monomers by free radical polymerization. The amount of NIPAAm utilized for polymerization was 0.290 g and was dissolved into 6 mL of D.I. water. Once dissolved, 62 µL of 0.1 M HCl solution was used to assist in pH adjustment of the monomer in solution. The pH was adjusted approximately to the pH of the H_2O_2 solution utilized during niosome formation. The HCl solution was acquired from Acros Organics (catalog number 124630010, 37% solution in water) and further diluted with D. I. water to achieve desired concentration.

Solutions of 0.005g/mL, 0.01g/mL, 0.02g/ mL, 0.025g/mL, and 0.04g/mL of BisAAm were made and the use of 34 µL of each was required in the polymerization of NIPAAm. Solutions of the initiator were made consisting of 0.1 g of APS in 1 mL of D.I. water. The amount of APS solution used in the polymerization process was 11.44 µL. The activator, TEMED, is a liquid solution and 36 µL were used. Once the monomer was dissolved into D.I. water, the process in which the remaining chemicals were utilized is as follow:

- HCl Solution
- BisAAm Solution
- APS Solution
- TEMED Solution

All samples were purged with nitrogen for five minutes after the addition of BisAAm solution and ten minutes after the addition of TEMED. Purging the samples

with nitrogen assisted in the removal of oxygen. Samples were left to polymerize for approximately 8 hours at room temperature.

3.3 Cell Potential Experiments versus Time

A cell stack comprised of six cells was utilized to run cell potential experiments as shown in Figure 12. The cell was manufactured from ABS plastic at SRI International [42]. Individual cells each had a volume of 65mL. The aluminum anode's dimension is 3.81 cm by 8.26 cm displayed in Figure 11. Different aluminum purities were utilized: 99.90%, 99.99%, and 99.998%. The aluminum foil of purity 99.90% was acquired from aluminum, catalog number 1145H. The aluminum foil of purity 99.99% and 99.998% were purchased from Alfa Aesar, catalog numbers are 40760 and 44492 respectively. An aqueous solution of NaOH was the electrolyte selected. Solutions were prepared with the use of NaOH (food grade) purchased from AAA Chemicals. A dielectric material (Polyester; with the same dimension as the anode) separates the anode from a thin silver electrode (catalyst electrode utilized) and prevents short circuiting within the cell.

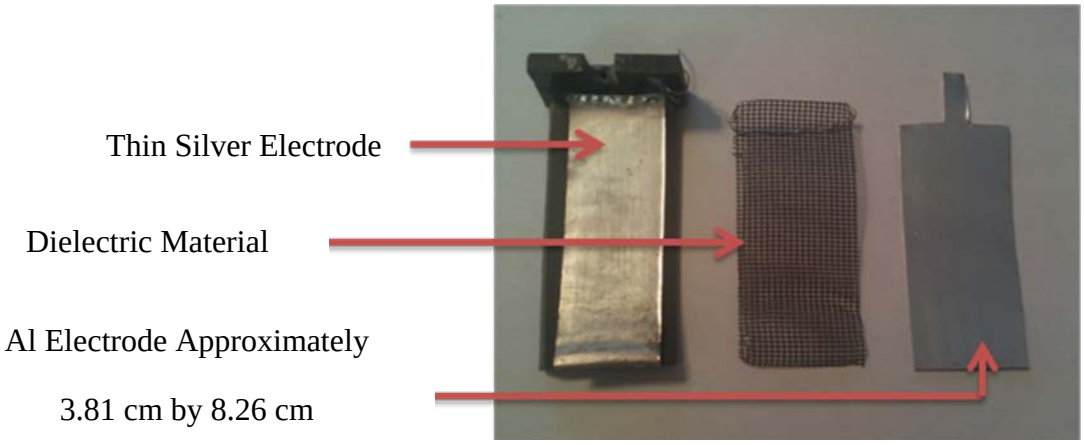

Figure 11: Electrodes and Dielectric Material

A Fluke 189 True RMS Multimeter was used to collect cell potential data during experimental runs. Data was collected until a value of 0.60 volts was achieved. For each experiment 2 mL of the encapsulated hydrogen peroxide solution and 45 mL of 1 M NaOH solution were utilized. The NaOH was first introduced into the cell followed by the hydrogen peroxide solution and data collection began. For experiments consisting of the use of polymers, the 2 mL hydrogen peroxide solution was mixed in the polymer container and allowed to sit for ten minutes to ensure diffusion of niosomes and H_2O_2 molecules into polymer before each experiment as shown in Figures 13 and 14. The polymer and niosome solution was further placed into the cell after the ten minutes and 45 mL of the 1 M NaOH solution was added. Once NaOH was in the cell, data collection commenced.

A.)

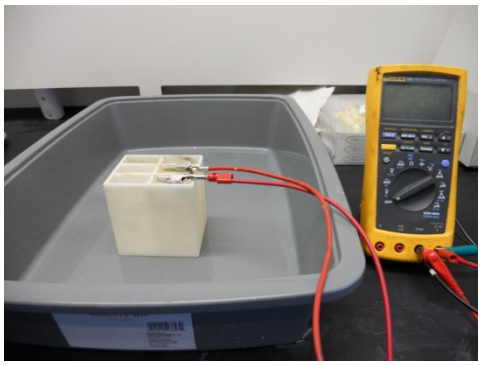

B.)

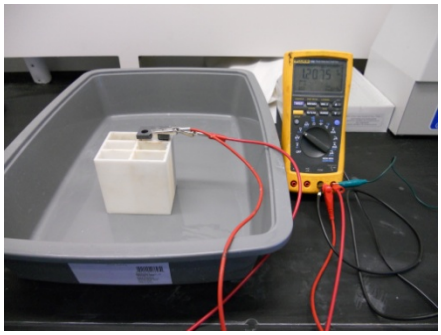

C.)

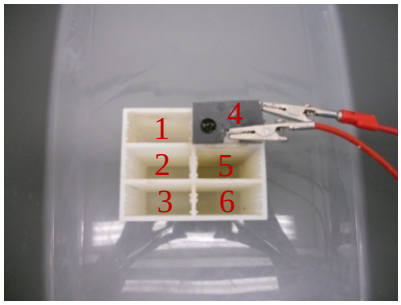

Figure 12: A.) Figure of Experimental Setup at Cell Position 6; B.) Figure of Experimental Setup at Cell Position 4; C.) Top View of Cell Stack with Numbered Cells

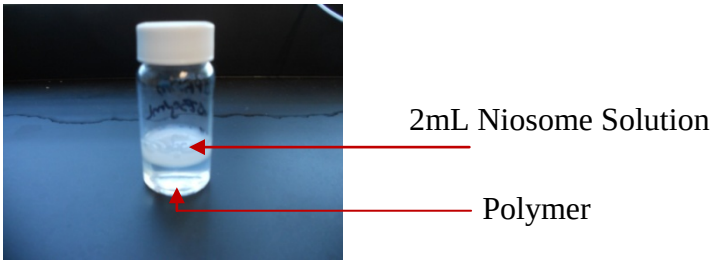

Figure 13: Polymer before Mixing Niosome Solution, Clear Separation

Figure 14: Polymer after Mixing Niosome Solution

Chapter 4: Results and Discussion

4.1 Niosome Size Characterization

4.1.1 Niosome Size Distribution Study

Particles in solution undergo a random displacement due to collisions amongst other particles, solvent molecules, or by an external force. The displacement of particles and molecules due to these collisions is termed Brownian motion [43]. To measure this displacement, a small region of a sample is illuminated and scattered light is detected. As the particles or molecules are in motion, there are fluctuations in light. Obtaining light fluctuations versus time results in the particles or molecules displacement in a small region. This information can be related to the rate of diffusion of molecules in and out of the small region. Applying the relationship between diffusion and particle size derived by Albert Einstein, hydrodynamic diameters (defined as the diameter for the particles in solution) can be obtained. This technique for measuring the diameter of particles in solution is termed dynamic light scattering (DLS) and was utilized to determine the size distribution of the niosomes in solution [43].

The methodology used to form niosomes incorporates extrusion with the goal of achieving a uniform size distribution among the niosome solution. We have hypothesized that by having a uniform size distribution of niosomes in the cell, amounts of hydrogen peroxide being released, by rupturing niosomes, will be similar throughout a cell's operational time. The first step in confirming this hypothesis is obtaining the size

distribution of niosomes after extrusion. Three batches of SPAN 60 niosomes encapsulated with 30% wt of H_2O_2 and resuspended into 30% wt of H_2O_2 solution (having a volume ratio of 0.25 as explained in section 3.1) were prepared and the niosomes' hydrodynamic diameter distribution was obtain by a Zetasizer Nano-S (Marvin,PA). Measurements were conducted on the day of preparation. Samples were prepared as follow: 100 µL of SPAN 60 niosome solution, described above, was further diluted into 900 µL of 30% wt of H_2O_2 solution. Three samples per batch were tested and their average size distribution is shown in Figures 15, 16, and 17. Reviewing results obtained by the DLS apparatus indicate that a uniform size distribution is not achieved after the niosomes have been extruded. In addition, the size distribution for each of the three batches is inconsistent with each other. The smallest range for niosome diameter is approximately 350 to 1500 nm (Batch 1). The largest range for niosome diameter is approximately 700 to 3500 nm (Batch 3). Imaging was conducted with a transmission electron microscope (TEM) of Batch 3 (largest niosome size distribution) and displayed in Figures 19 and 20. All imaging was conducted within 24 hours of niosome preparation. Figure 19 exhibits niosomes in the lower end of the size distribution curve. Figure 20 exhibits niosomes in the upper end of the size distribution curve.

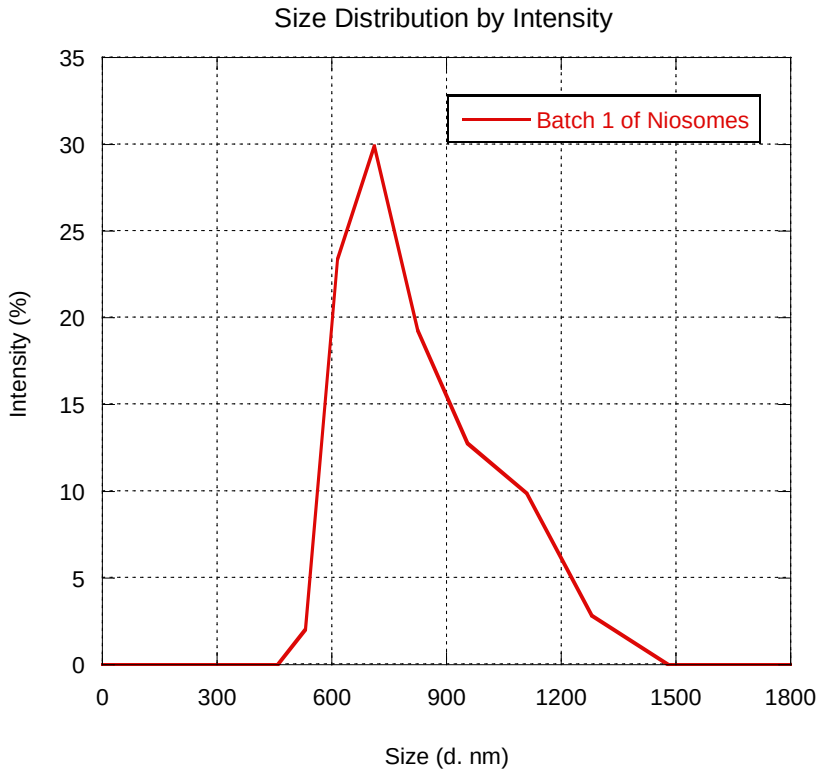

Figure 15: Size Distribution for SPAN 60 Niosomes: Batch 1; Measurement Taken on the Day Niosomes were Prepared

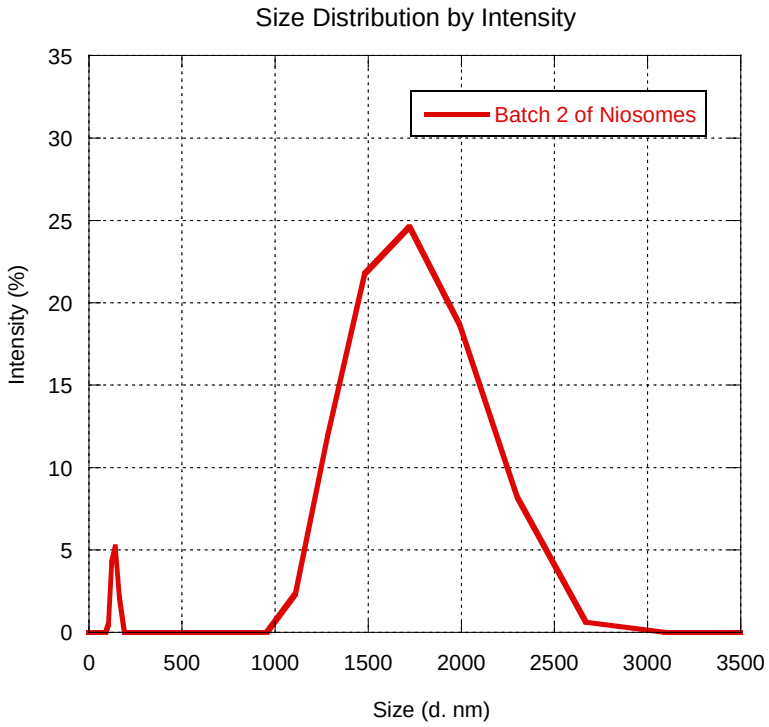

Figure 16: Size Distribution for SPAN 60 Niosomes: Batch 2; Measurement Taken on the Day Niosomes were Prepared

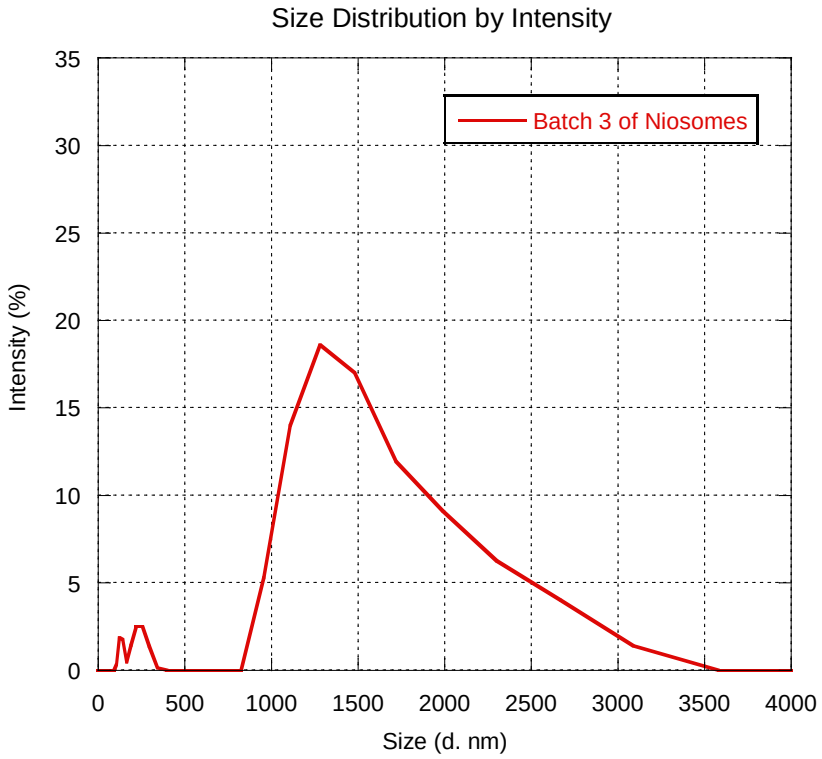

Figure 17: Size Distribution for SPAN 60 Niosomes: Batch 3; Measurement Taken on the Day Niosomes were Prepared

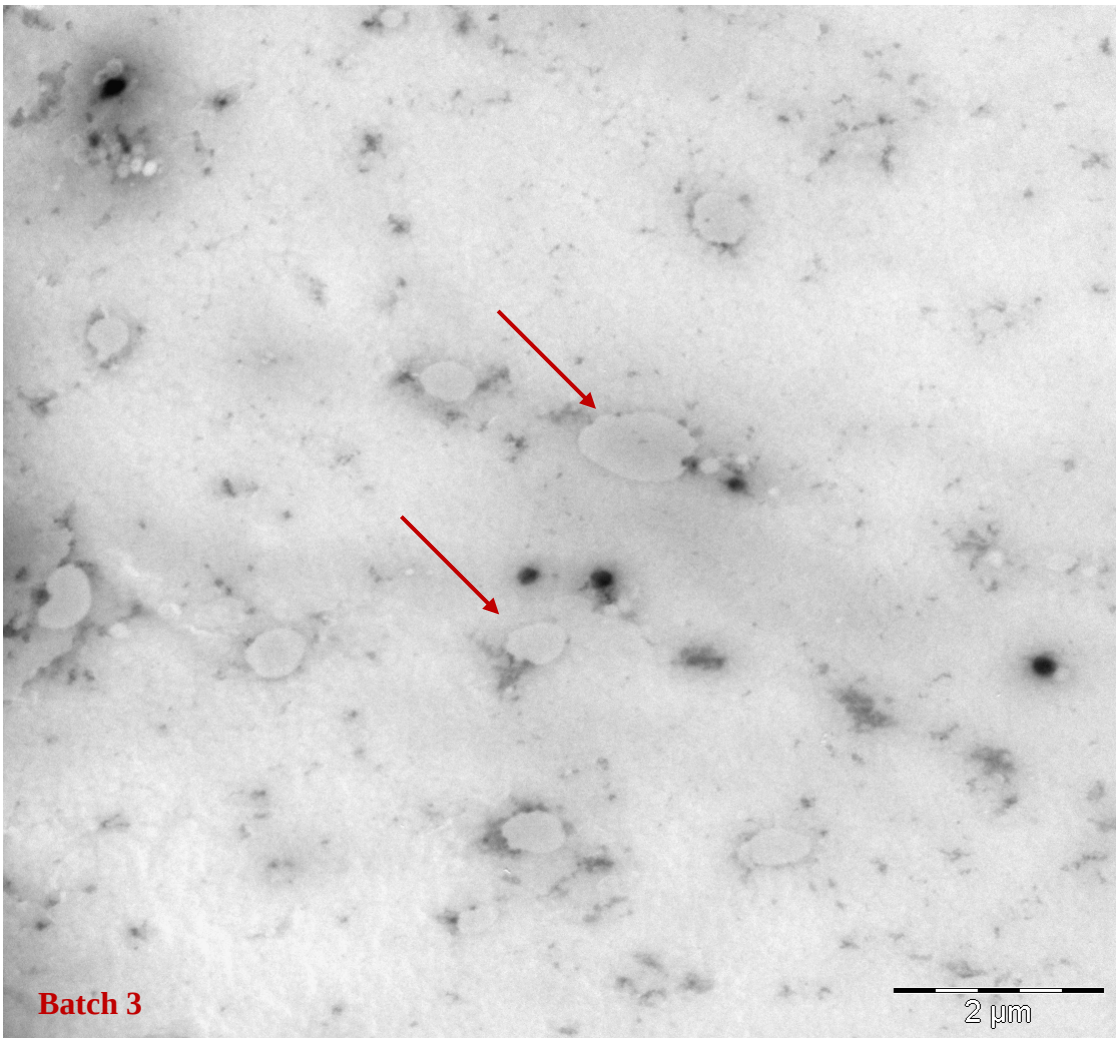

Figure 18: TEM Image of Sample from Batch 3 (SPAN 60 Niosomes) at 7.1KX Magnification: Image Displays Niosomes on the Lower End of the Size Distribution Curve Shown in Figure 17

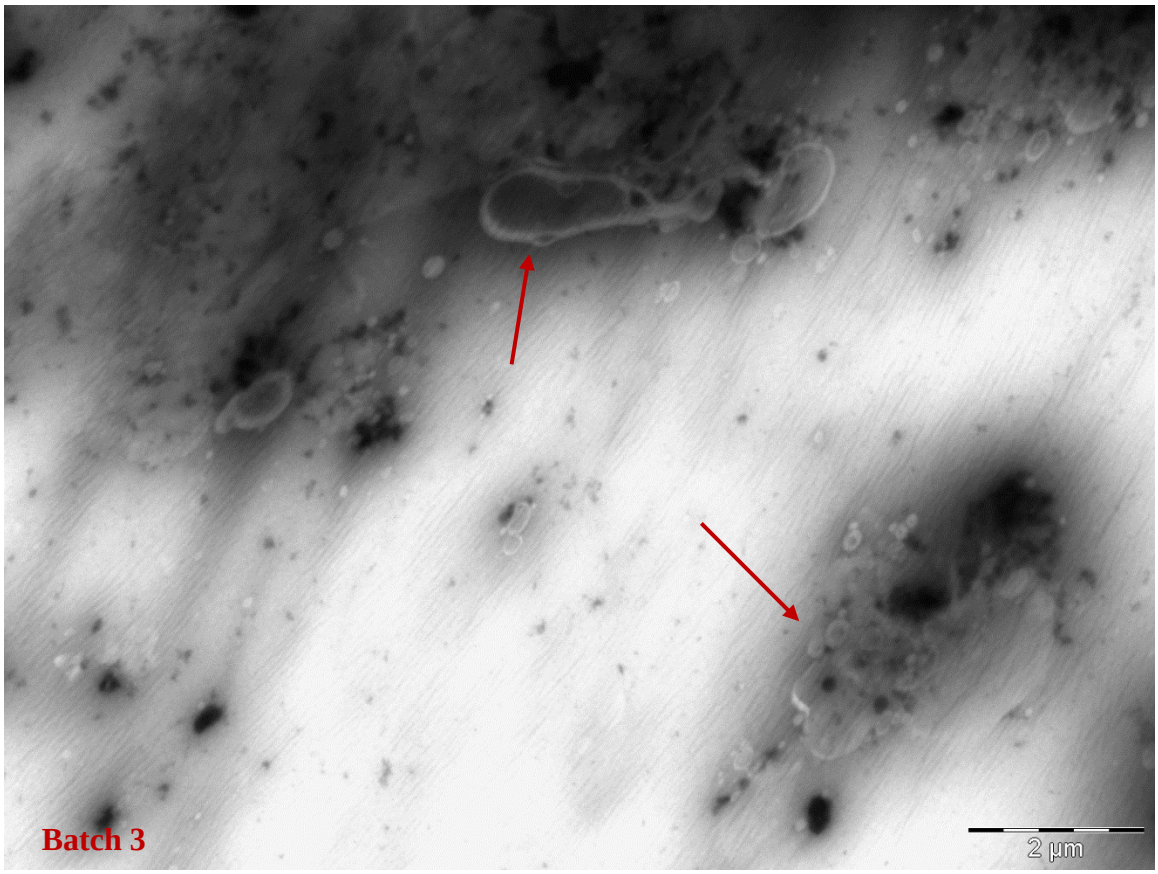

Figure 19: TEM Image of Sample from Batch 3 (SPAN 60 Niosomes) at 7.1KX Magnification: Image Displays Niosomes on the Upper End of the Size Distribution Curve Shown in Figure 17

4.1.2 Dynamic Behavior of Niosome's Diameter for Long Term Stability

To further assess niosome size distribution after extrusion, the previous niosome batches, discussed in section 4.1.1, were monitored versus time. Only the highest intensity reading for fluctuation in light was considered as the niosomes' hydrodynamic diameter value. As an example of the highest intensity peak that will be considered as the niosomes' hydrodynamic diameter value refer to Figure 16. There are two intensity peaks for Figure 16, the average diameter of the particle in solution for the highest intensity peak will be considered as the niosomes' hydrodynamic diameter value utilized in the following investigation. Samples were prepared as follow: 100 µL of SPAN 60 niosome solution was further diluted into 900 µL of 30% wt of H_2O_2 solution. The reported niosome hydrodynamic diameter (diameter size with the highest intensity fluctuation in light) for each batch is an average of 3 readings taken from each batch on days 0, 3, 6, and 9. Results in Figure 20 indicate the niosomes in each different batch to be instable (due to the niosomes rupturing and reforming into different sized vesicles as time increases). Although Figure 20 suggest that the niosomes converge to a similar size after 9 days, further testing is required.

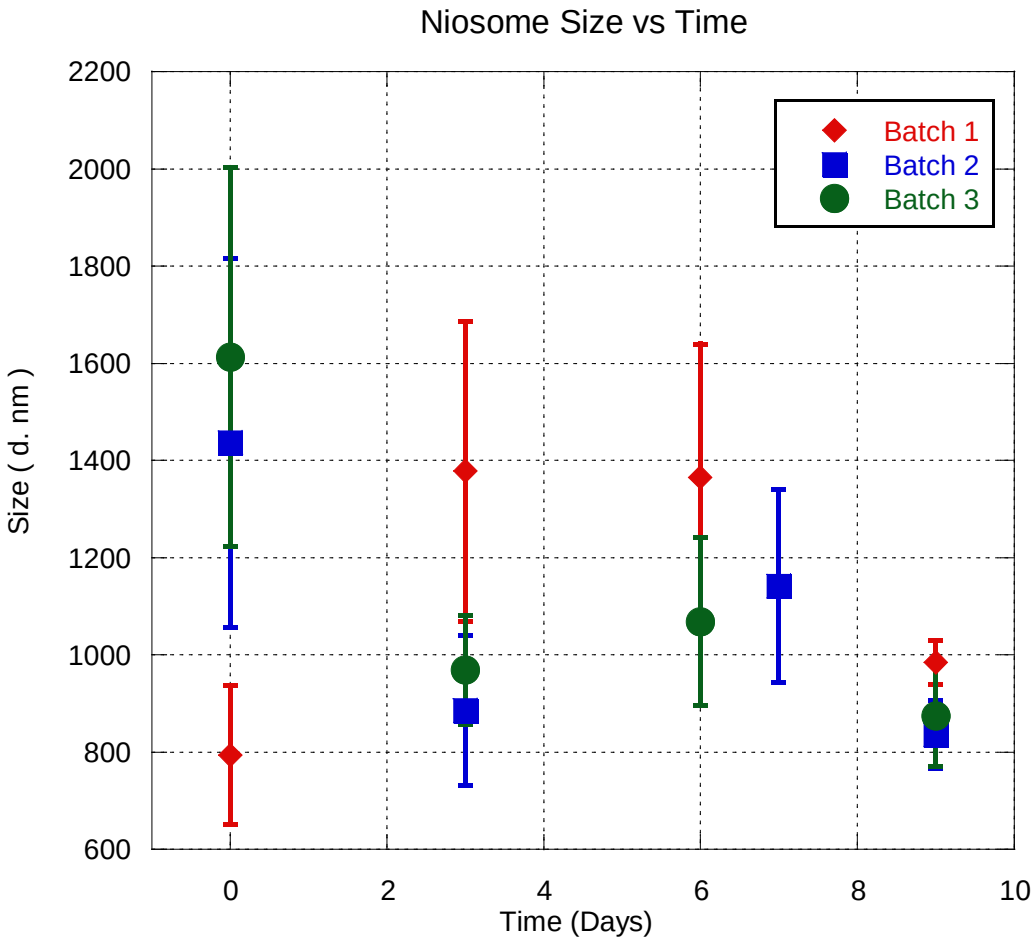

Figure 20: Niosomes' Hydrodynamic Diameter versus Time for Batch 1, 2, & 3

4.1.3 Niosome Size Distribution Before and After Extrusion

Results from section 4.1.1 conclude that a uniform size distribution of niosomes is not achieved after the extrusion process. A study was conducted to determine niosome size distribution before and after extrusion. After the hydration of the thin film is accomplished during niosome preparation, the niosome solution is sonicated for ten minutes. Extrusion proceeds after sonication. For this study (effects of extrusion to niosome size distribution), niosomes are suspended into 30% wt hydrogen peroxide solution (having a volume ratio of 0.25 explained in section 3.1). Two different niosome batches were prepared and measurements for niosome size distribution before and after extrusion were obtained. Samples were prepared as follow for DLS measurements: 100 µL of SPAN 60 niosome sonicated solution was further diluted into 900 µL of 30% wt of H_2O_2 solution. Results acquired were unexpected, indicating a more uniform distribution of size before the extrusion of niosomes as shown in Figures 21 and 22. During the extrusion process, niosomes are forced through a porous membrane of 0.08 micrometer pore size. They are forced to rupture and reform into vesicles. With enough passes through the membrane, niosomes are believed to reform into small enough vesicles that will pass through the membrane without rupturing. However, we have hypothesized that the niosomes are potentially aggregating and as a result different size distribution profiles are achieved. It is a possibility that the membrane pore size is not properly adequate for encapsulated H_2O_2 niosome extrusion. Further investigation is required to properly assess size distribution before and after extrusion that would incorporate additional niosome batches, measurements taken before sonication, and altering membranes with

different pore sizes. Future work might indicate that the sonication of niosomes, excluding extrusion, might suffice and ultimately save future users time and money.

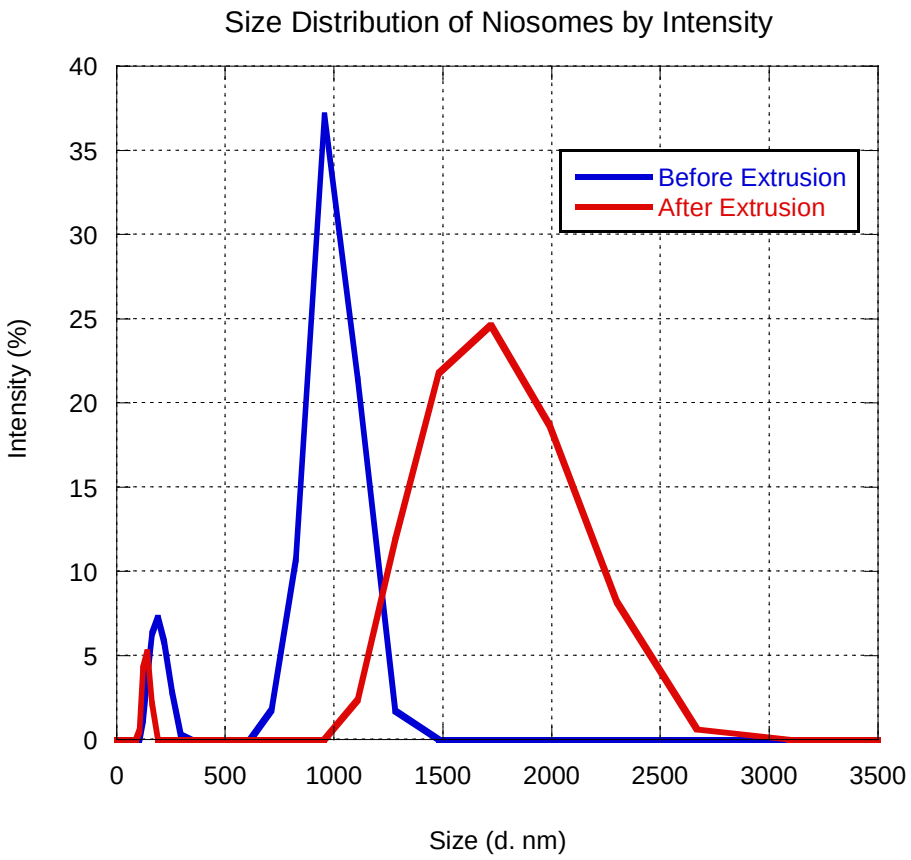

Figure 21: Size Distribution for Niosomes Before and After Extrusion; Batch 1

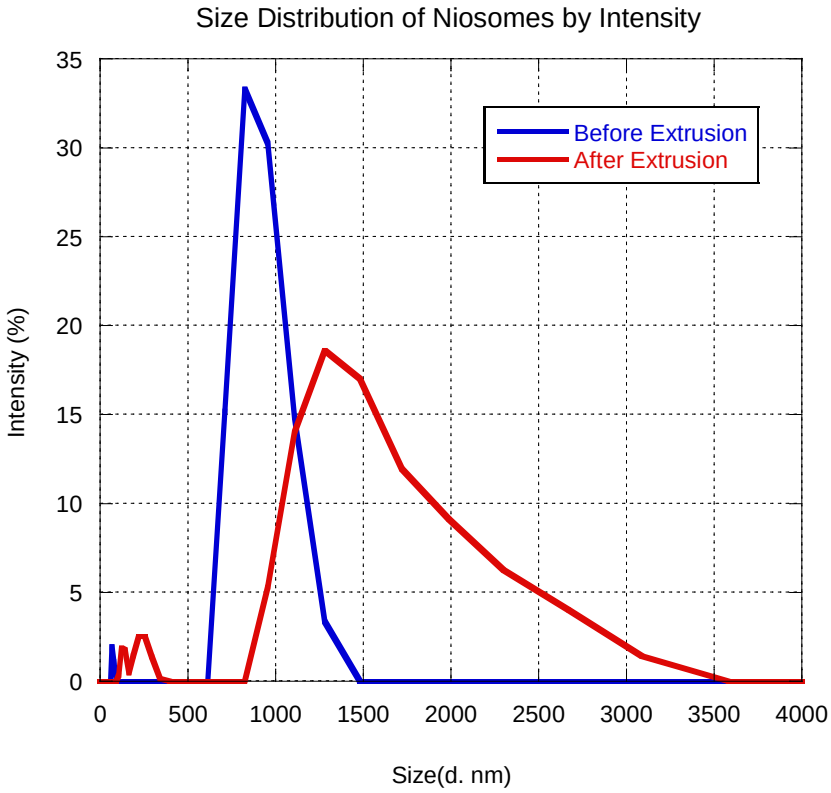

Figure 22: Size Distribution for Niosomes Before and After Extrusion; Batch 2

4.2 Investigation of Proposed System Compared to Traditional Al / H_2O_2 System

4.2.1 Premise of Investigation

In this study, experimental data was collected for four distinctive cases under a constant load of 10 ohms. The first case is set as a control (the use of H_2O_2 solution only) to monitor and compare the effectiveness of the proposed cathodic control system. The second case utilizes the niosomes suspended in the same weight percentage of H_2O_2 solution encapsulated inside the vesicles without being exposed to the polymer. Comparison between case number one and two will provide insight of the niosomes' contribution to the cell's characteristics, such as overall cell power output and aluminum consumption. The third case is niosomes implemented with the polymer (the proposed system). In the third case, niosomes in suspension are exposed to the polymer and are further mixed to ensure uniform exposure of the niosome solution. Cell characteristic values obtained for case three were compared to case two to acquire information in regards to the effects the polymer exposure created. Furthermore, case three was compared to case one (the control) and will assist in determining the effects that the proposed cathodic control system had to the cell's characteristics. Involving the use of the selected polymer provides the second control element over the release of H_2O_2. Case four was developed involving the exposure of H_2O_2 solution (without suspended niosomes) to the selected polymer and cell characteristic values obtained were compared against values for the proposed system. This comparison will provide insight as to the contribution the niosomes in the proposed system have on the cell's characteristics. A total of three replicates were conducted for each case (1-4) involved in the investigation.

The comparison of average obtained cell characteristic values to the control (case 1) was utilized to calculate percent change values for cases 2 through 4.

Both the corrosion of aluminum and decomposition of hydrogen peroxide consume material. The direct reaction of aluminum with hydrogen peroxide forms precipitates of aluminum hydroxide that forms a thin coating on the anode interfering with the electrochemical reaction. All three parasitic reactions hinder the electrical performance of the Al / H_2O_2 electrochemical cell. The aim for this investigation is to decrease parasitic reactions by implementing a novel methodology to control reagent release, in this case hydrogen peroxide.

4.2.2 Results from Investigation of Proposed System Utilizing Al Purity of 99.99%

The cell's operational times were recorded at the conclusion of each experimental run. The end of each experimental run is defined in this work when cell potentials reach 0.60 Volts. The integration of instantaneous power as a function of time divided by the cell's operational time results in the cell's overall power output, equation displayed in Table 1. There were five replicates achieved to provide an average overall cell power output value for the study incorporating aluminum purity of 99.99 % (with the exception of case 4 where three replicates were conducted). Figure 23 displays the results of all four cases previously explained. The comparison of average values to the control (case 1) was utilized to calculate percent change values, in all cell characteristics, for cases 2 through 4.

The introduction of niosomes in suspension to the system resulted in highest increase in power output compare to the control (case number one) with a 6 % increase in

the average value (0.126 W +/- 0.01 W and 0.119 W +/- 0.01 W respectively). Statistical significance testing (student's t-test) was conducted on experimental values obtained for the control against experimental values obtained for niosomes in suspension. The null hypothesis is that the two mean values for power output are the same. A two-sample t-test results in failure to reject the null hypothesis at the 5% significance level. The increase in power output value is attributed to the amount of work obtained with the utilization of niosomes in suspension in the Al / H_2O_2 electrochemical cell (0.606 KJ +/- 0.096 KJ with niosomes in suspension versus 0.542 KJ +/- 0.05 KJ value for control). This leads to indicate that the niosomes are successfully decreasing parasitic reactions that influence a cell's overall power generation (as time progresses the niosomes are rupturing and releasing hydrogen peroxide). The use of the polymer implemented with the niosomes caused a decrease of 8% compared to the control's average value (as well as the use of the polymer with no niosomes present). The decrease can be accounted by the overall cell power output equation in Table 1, where a cell's overall power output value is equal to the amount of work obtained divided by a cell's operational time. The average amount of work obtain with the novel proposed system is higher than the control's average amount of work (0.57 KJ +/- 0.09 KJ and 0.542 KJ +/- 0.05 KJ respectively) and the average cell operational time is higher by 13% (87 min +/- 12.1 min and 77 min +/- 12.4 min respectively, shown in Figure 24) causing the value in cell power to be lower compared to the control. Statistical significance testing (student's t-test) was conducted on experimental values obtain for the control against experimental values obtained for the proposed system for energetic values. The null hypothesis is that the two mean values for energy output are the same. A two-sample t-test results in failure to reject the null

hypothesis at the 5% significance level. The presence of niosomes in the novel proposed system increases the average amount of work obtained versus the use of the polymer without niosomes (0.57 KJ +/- 0.09 KJ and 0.52 KJ +/- 0.047 KJ respectively). Results support aim of consuming material adequately by reducing parasitic reactions.

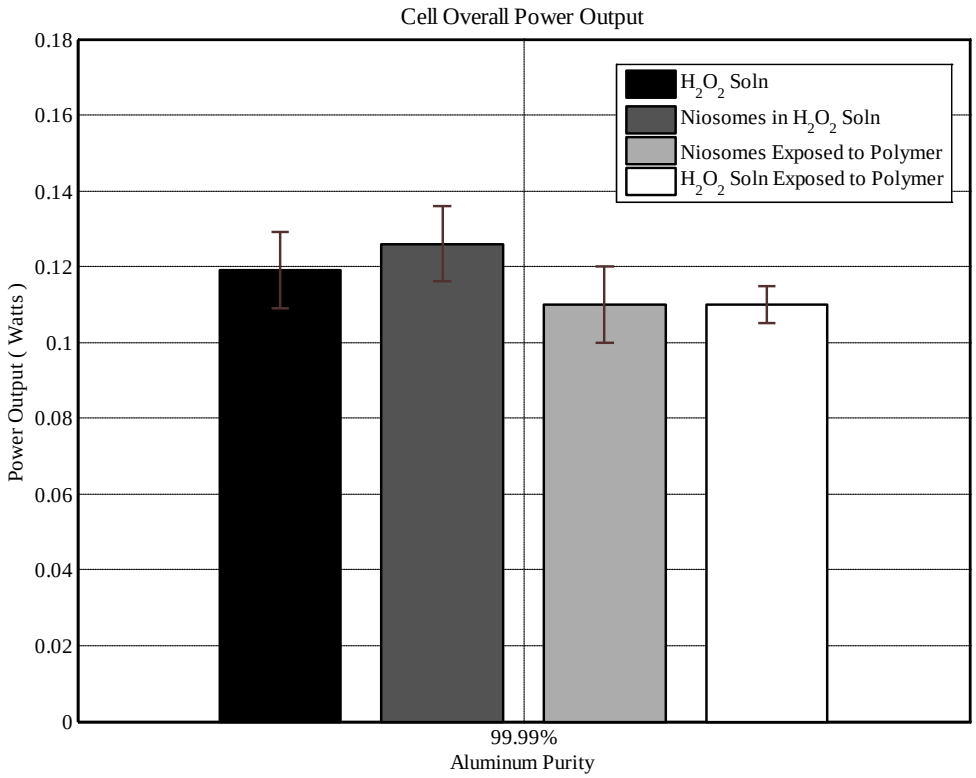

Figure 23: Average Cell Overall Power Output Utilizing Al Purity 99.99%

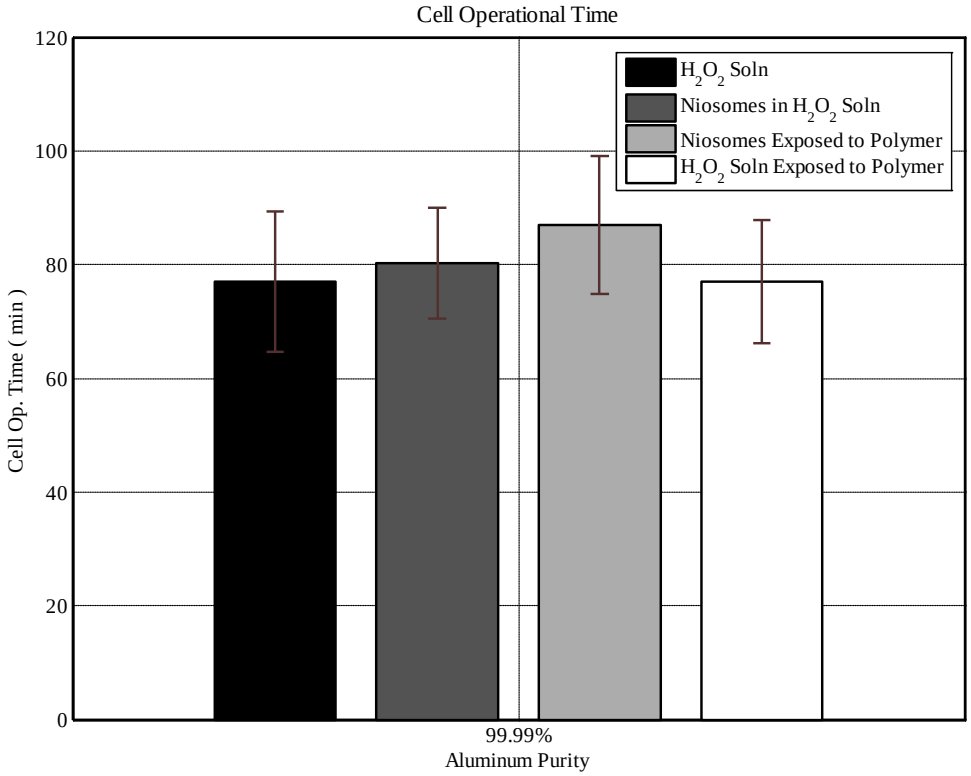

Figure 24: Average Cell Op. Times Utilizing Al Purity 99.99%

Before and after each experimental run, the aluminum electrode's mass was acquired to determine aluminum consumption. Increasing power generation by reagent control via encapsulation and further exposure to a polymer is this works' aim with consideration of aluminum consumption. Lowering aluminum consumption results in material conservation and prolongs the utilization of the cell. Reviewing average aluminum consumption results show a 10% increase in the use of niosomes in suspension (without polymer) compared to the control. This increase is expected due to the increase in the cell's overall average power output value shown in Figure 23 (12% increase in obtained work value compared to the control). There is a decrease of 15% in aluminum

consumption with the proposed novel system (niosomes exposed to the polymer). Results confirm that the presence of niosomes is attributed to the decrease in aluminum consumption. This statement is supported by comparing aluminum consumption values between the novel proposed system and the use of a polymer without the presence of niosomes in a Al / H_2O_2 electrochemical cell. Results for the novel proposed system in Figure 25 supports the aim of lowering aluminum consumption for material conservation that will in return prolong the utilization of the cell.

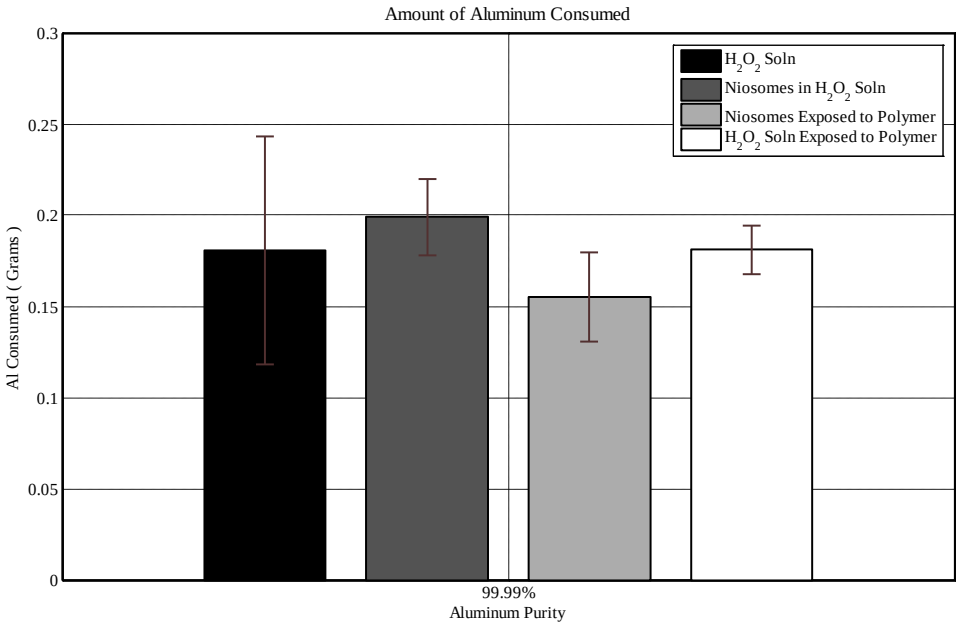

Figure 25: Average Al Consumption Values Utilizing Al Purity of 99.99%

In order to assess the effects of implementing niosomes and a polymer into an aluminum anode H_2O_2-alkaline electrochemical cell, the energetic output was determined by utilizing the equation for work in Table 1. Calculating energy and dividing by grams of aluminum consumed is a ratio providing an evaluation of the cell's performance. An

increase in this value is encouraged, indicating an increase in energy or a decrease in aluminum consumption. Introducing niosomes into the system did not result in a significant increase in the average value (energy per gram of Al consumed) as illustrated in Figure 26. Utilizing the novel proposed system (polymer implemented with suspended niosomes) resulted in an increase in energy per gram of aluminum consumed due to the 15% decrease in the average aluminum consumption value (compared to the control's average value) observed in Figure 25.

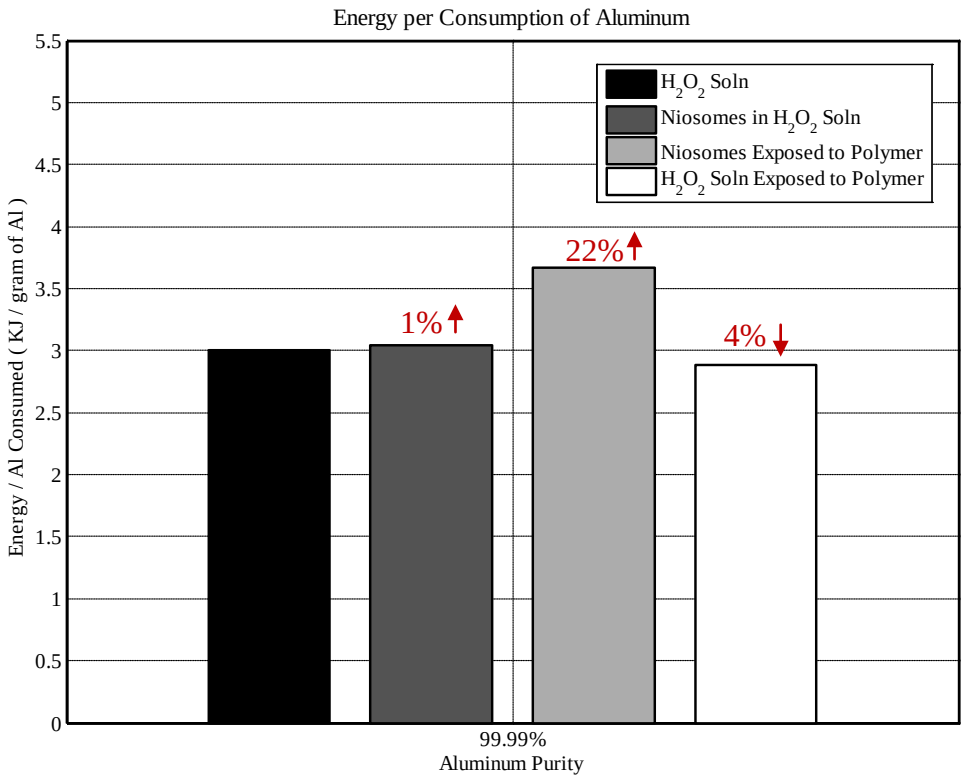

Figure 26: Energy per Al Consumed in Grams Utilizing Al Purity of 99.99% (Numbers in Red Indicated Percent Change Compared to Control)

4.2.3 Comparison of Cell Characteristics between SPAN 40 and SPAN 60 Composed Niosomes

The following investigation was conducted to determine the effects altering the surfactant would have on the cell characteristics. The work that has been currently presented involves the use of Sorbitan Monostearate (SPAN 60) as the non-ionic surfactant incorporated in niosome formation. In the following investigation utilizing aluminum purity 99.99%, as in the previous results above, the non-ionic surfactant component is altered to Sorbitan Monopalmitate (SPAN 40). Differences between SPAN 40 and 60 arise in the length of the hydrophobic hydrocarbon chain in the niosome's composition. The use of SPAN 40 theoretically results in smaller niosomes due to a shorter chain length compared to SPAN 60 (molecular structure shown in Figure 5). An investigation was conducted to determine the effects SPAN 40 versus SPAN 60 would have on the systems in this study. The SPAN 40 niosomes were formed following the same procedure conducted for SPAN 60 niosomes with replacing the non-ionic surfactant component. The number of moles for SPAN 60 was equaled to the number of moles for SPAN 40 used in the niosome preparation procedure. The amount of cholesterol and DCP for both SPAN 60 and 40 niosomes remained constant. Two cases were developed and tested. In the first case, the niosomes are suspended in the same weight percentage of H_2O_2 solution encapsulated inside the vesicles (having a volume ratio of 0.25 explained in section 3.1). Case number two, involves the use of the proposed system where suspended niosomes are exposed to the selected polymer [poly(N-isopropylacrylamide)] for control of cathodic reagent release. For figures 29-31, results from the use of niosomes with non-ionic surfactant SPAN 40 are displayed in aqua blue and SPAN 60 in

dark grey. A total of five replicates were conducted for each case involved in the investigation.

Size distribution curves were obtained for SPAN 40 and 60 niosomes utilized. Size distribution data was obtain by a Zetasizer Nano-S (Marvin,PA). Measurements were conducted once niosome preparation concluded. Samples were prepared as follow: 100 µL of SPAN 40/60 niosome solution, described above, was further diluted into 900 µL of 30% wt of H_2O_2 solution. Two samples per batch were tested and their average size distribution is shown in Figures 27 and 28. Results for SPAN 60 niosomes are consistent with results discussed in section 4.1.1, where a non-uniform size distribution is not achieved once niosome are extruded. In addition, the range of niosome diameter for SPAN 60 niosomes are inconsistent compared to each batch measured. Size distribution curves obtained for SPAN 40 niosomes display a non-uniform distribution of size likewise, shown in Figure 28. In comparison to SPAN 60 niosomes, the range of niosome diameter for SPAN 40 niosomes is considerably greater. This is an indication that SPAN 40 niosomes are instable. Furthermore, it is hypothesized that SPAN 40 niosomes might be aggravating and alterations to DCP amounts will assist in the prevention of aggravation. Size distribution results for SPAN 40 niosomes indicate further investigation is require for proper niosome size characterization. In addition, an improvement upon SPAN 40 niosome preparation procedure is deemed necessary evident from its large size distribution, refer to Figure 27.

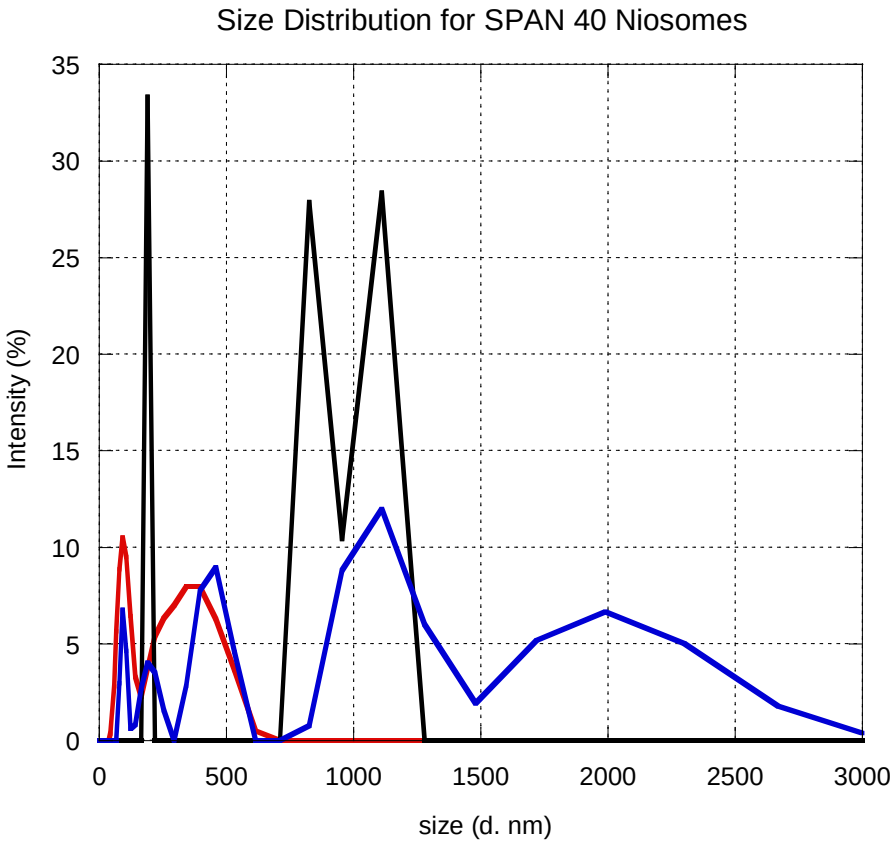

Figure 27: Size Distribution Curve for SPAN 40 Niosomes (Three Different Batches) Utilized in SPAN 40 vs. 60 Niosome Experiments

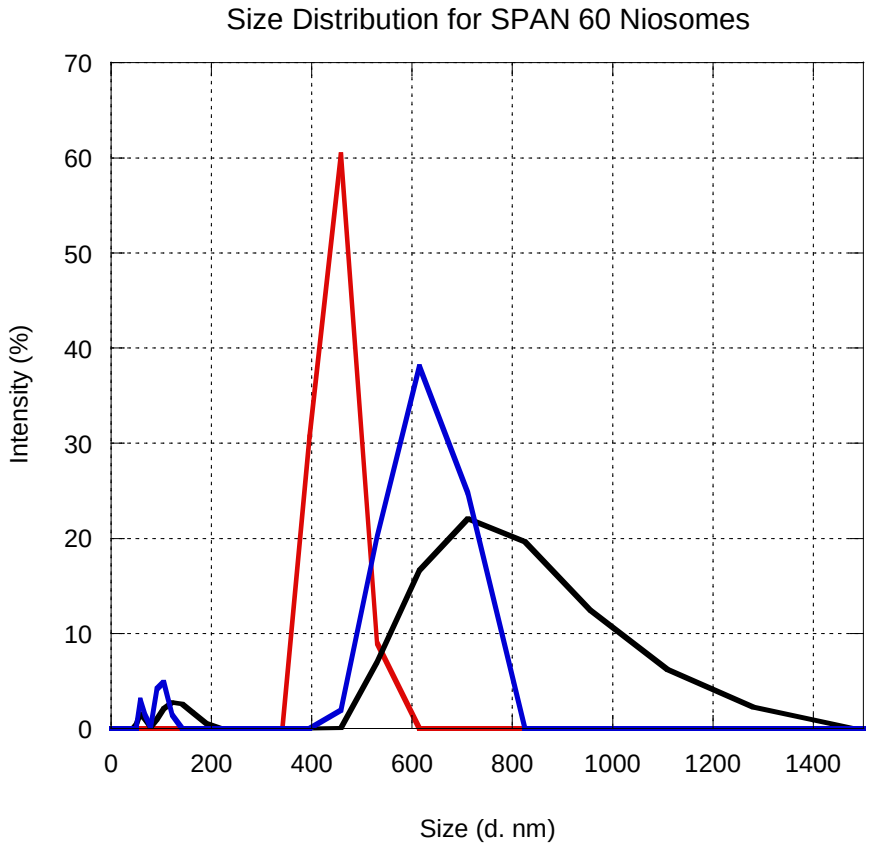

Figure 28: Size Distribution Curve for SPAN 60 Niosomes (Three Different Batches) Utilized in SPAN 40 vs. 60 Niosome Experiments

For comparison purposes, percent difference in values between results for SPAN 40 niosomes and SPAN 60 niosomes utilized average cell characteristic values. The use of SPAN 60 niosomes in case one proves to outperform SPAN 40 niosomes in overall cell power output with an average value of 0.126 Watts +/- 0.01 W compared to 0.11 Watts +/- 0.02 (14% difference in power generation value from utilizing SPAN 40 versus SPAN 60, refer to Figure 29). This difference may be attributed to SPAN 60 niosomes rupturing at a slower rate compared to SPAN 40 niosomes. There was no difference observed in power output values between the use of SPAN 40 niosomes or SPAN 60 niosomes for the novel proposed system. Both produced the same average value for the

amount of work of 0.57 KJ +/- 0.09 KJ and similar cell operational time values likewise (Figure 30).

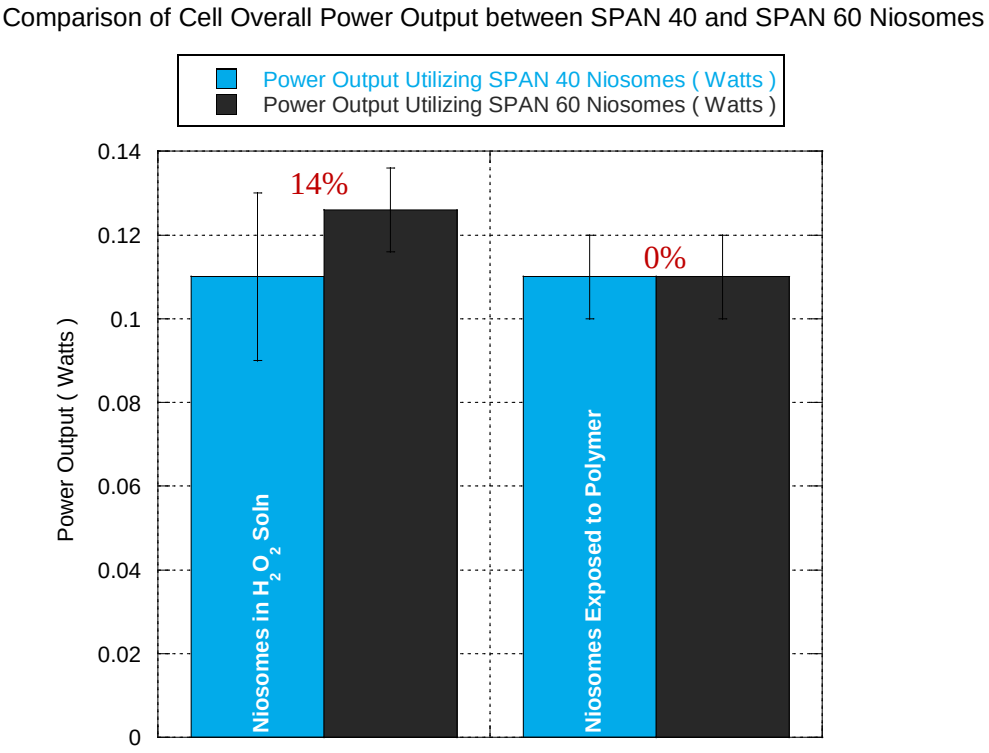

Figure 29: Average Power Output Utilizing Al Purity 99.99%, SPAN 40 vs. SPAN 60 Niosomes (Numbers in Red Indicated Percent Difference between Values)

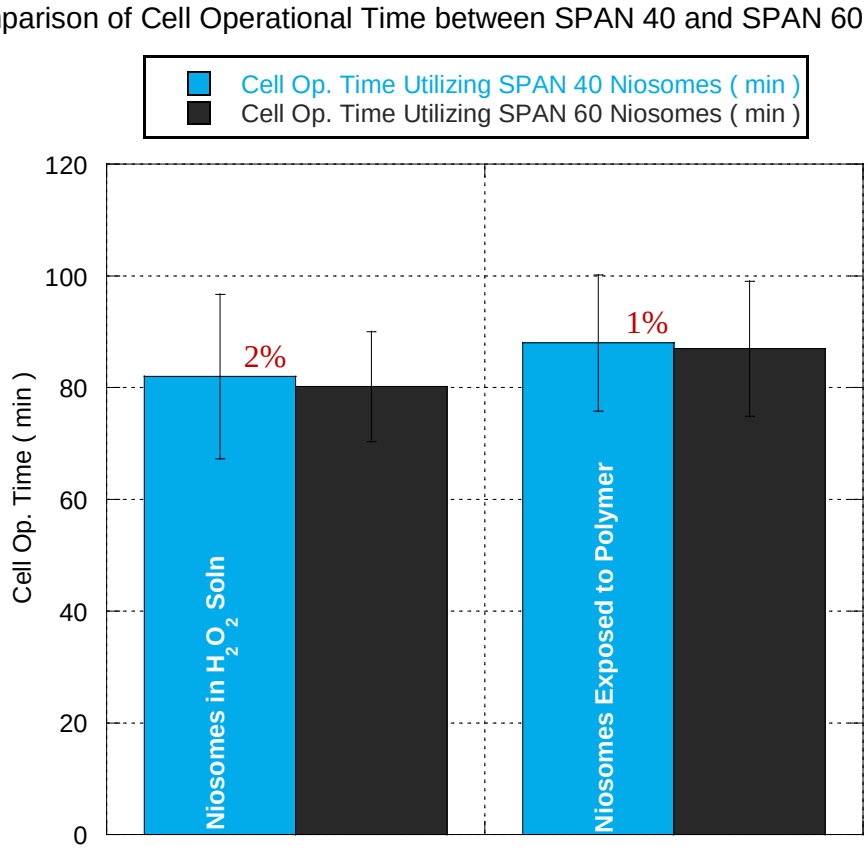

Figure 30: Average Cell Op. Time Utilizing Al Purity 99.99%, SPAN 40 vs. SPAN 60 Niosomes (Numbers in Red Indicated Percent Difference between Values)

Differences arise in aluminum consumption values between SPAN 40 and SPAN 60 niosomes. For case one, where niosomes in suspension was investigated, SPAN 40 niosomes consumed less aluminum compared to niosomes composed of SPAN 60 surfactant. The difference in average aluminum consumption values was expected due to the higher amount of work obtained from the use of SPAN 60 niosomes versus SPAN 40 niosomes (0.606 KJ +/- 0.096 KJ and 0.51 KJ +/- 0.091 respectively). The percent difference between both aluminum consumption values is approximately 12%. In the utilization of the proposed system, the percent difference between Al consumption values is 7%. Statistical significance testing (student's t-test) was conducted on experimental

aluminum consumption values obtain for SPAN 40 and SPAN 60 niosomes incorporated in the proposed system. The null hypothesis is that the two mean values for aluminum consumption are the same. A two-sample t-test results in failure to reject the null hypothesis at the 5% significance level. Although similar cell operational time and discrete work values were observed, SPAN 60 niosomes were successful in reducing parasitic reactions due to the difference in aluminum consumption (Figure 31).

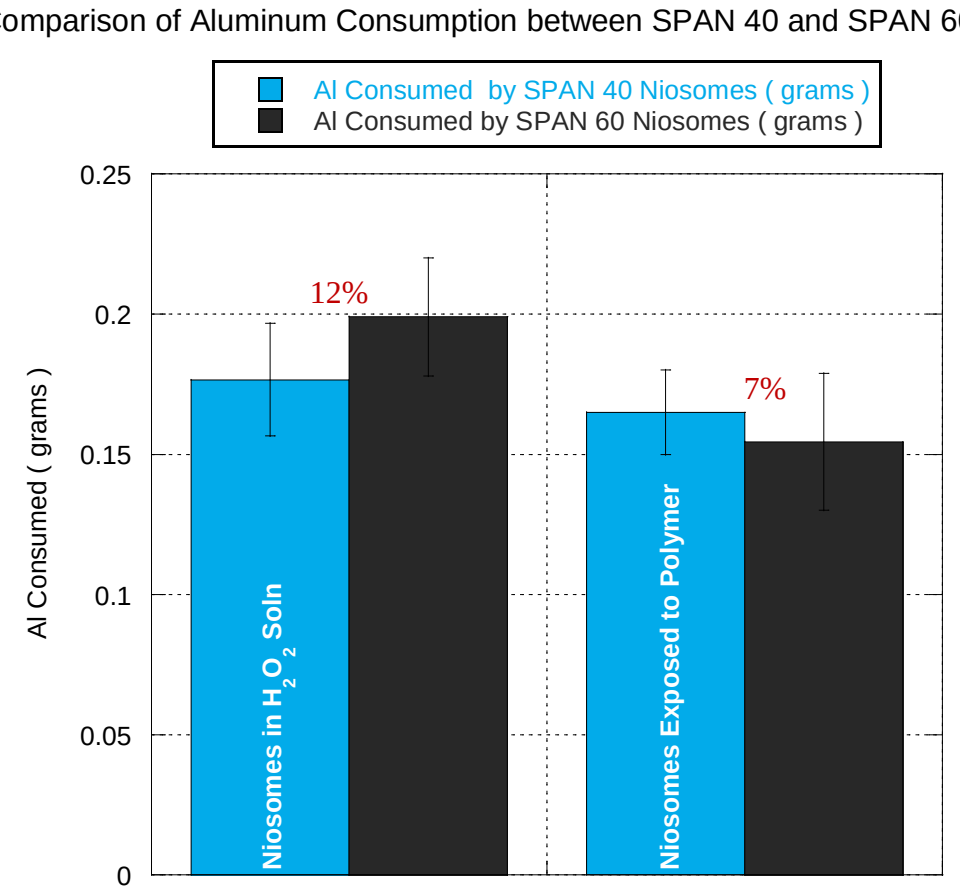

Figure 31: Average Al Consumption Utilizing Al Purity 99.99%, SPAN 40 vs. SPAN 60 Niosomes (Numbers in Red Indicated Percent Difference between Values)

Evaluating the ratio of energy per gram or dollar of aluminum consumed for the presence of niosomes suspended in solution between the use of SPAN 40 and 60 niosomes resulted in a 6% difference in value (percent difference in value calculated with the use of data acquired from Tables 3 and 4). The ratio of energy per gram or dollar of aluminum consumed for the proposed system with the use of SPAN 40 and SPAN 60 as the surfactant component resulted in a 5% difference in value (% difference values calculated with the use of data acquired from Tables 3 and 4). Due to low percent differences in energy per gram or dollar of aluminum consumed ratios between using SPAN 40 versus SPAN 60 niosomes, the utilization of either is adequate (exclusively based on these two ratio parameters).

Table 3: Amount of Energetic Output per Amount of Al Consumed for Niosomes in Suspension (Without Polymer)

Work / Al Consumed :	KJ / g of Al Consumed	KJ / $ of Al Consumed
SPAN 40 Nio.	2.87	0.205
SPAN 60 Nio.	3.04	0.217

Table 4: Amount of Energetic Output per Amount of Al Consumed for Novel Proposed System

Work / Al Consumed :	KJ / g of Al Consumed	KJ / $ of Al Consumed
SPAN 40 Nio.	3.48	0.248
SPAN 60 Nio.	3.67	0.262

4.2.4 Comparison of Different Aluminum Purities on Proposed System

Another factor influencing electrochemical cell's characteristics is the purity of the aluminum anode. To determine the effects of altering aluminum purity, the following investigation, resembling the experimental set up in 4.2.2, was conducted utilizing aluminum purities of 99.998%, 99.99%, and 99.90%. Experimental data was collected for four distinctive cases under a constant load of 10 ohms. The first case is set as a control (the use of H_2O_2 solution only) to monitor and compare the effectiveness of the proposed cathodic control system. The second case utilizes the niosomes suspended in the same weight percentage of H_2O_2 solution encapsulated inside the vesicles without being exposed to the polymer. Comparison between case number one and two will provide insight of the niosomes' contribution to the cell's characteristics, such as overall cell power output and aluminum consumption. The third case is niosomes implemented with the polymer (the proposed system). In this case, niosomes in suspension are exposed to the polymer and are further mixed to ensure uniform exposure of the niosome solution. Cell characteristic values obtained for case three were compared to case two to acquire information in regards to the effects the polymer exposure created. Furthermore, case three was compared to case one (the control) and will assist in determining the effects that the proposed cathodic control system had to the cell's characteristics. Involving the use of the selected polymer provides the second control element over the release of H_2O_2. Case four was developed involving the exposure of H_2O_2 solution (without suspended niosomes) to the selected polymer and cell characteristic values obtained were compared against values for the proposed system. This comparison will provide insight as to the contribution the niosomes in the proposed system have on the cell's characteristics. A

total of three replicates were conducted for each case (1-4) involved in the investigation on the influence of aluminum purities on the cell's characteristics. The comparison of average obtained cell characteristic values to the control (case 1) was utilized to calculate percent change values for cases 2 through 4.

Overall average cell power output values were highest amongst all experimental cases and aluminum purities for the use of niosomes in suspension (without exposure to a polymer). This is attributed to the niosomes achieving higher average work values compared to the control, the proposed system, and the use of the polymer without niosomes present. Percent change values, in comparison between the control to all three cases, were highest for aluminum purity of 99.998% when reviewing average work values and average cell operational times (refer to Figure 34). With the exception of case three, aluminum purity of 99.998% had the highest increase in value for energy per gram of aluminum consumed (Figure 35). Niosomes in suspension (without exposure to a polymer) for aluminum purity of 99.998% had a 12% increase in overall average power output value, compared to the average value for the control, and was the highest increase among the three different aluminum purities as reported in Figure 32. In consequence, the use of niosomes in suspension achieved the highest increase of aluminum consumption likewise (Figure 33).

Average aluminum consumption values for aluminum purity of 99.90% significantly decrease by 32 % (compared to the control) with the use of the novel control reagent release system (niosomes exposed to a polymer) and the polymer without the presence of niosomes (H_2O_2 solution exposed to a polymer) and by 9.8% with the use of niosomes in suspension shown in Figure 33. Thus far, experimental cases with the

highest average power output value have the highest aluminum consumption. This trend is evident in comparing Figures 32 and 33 for aluminum purities of 99.998% and 99.99% however, aluminum purity of 99.90% behaves otherwise. For this purity the control consumed the greatest amount of aluminum.

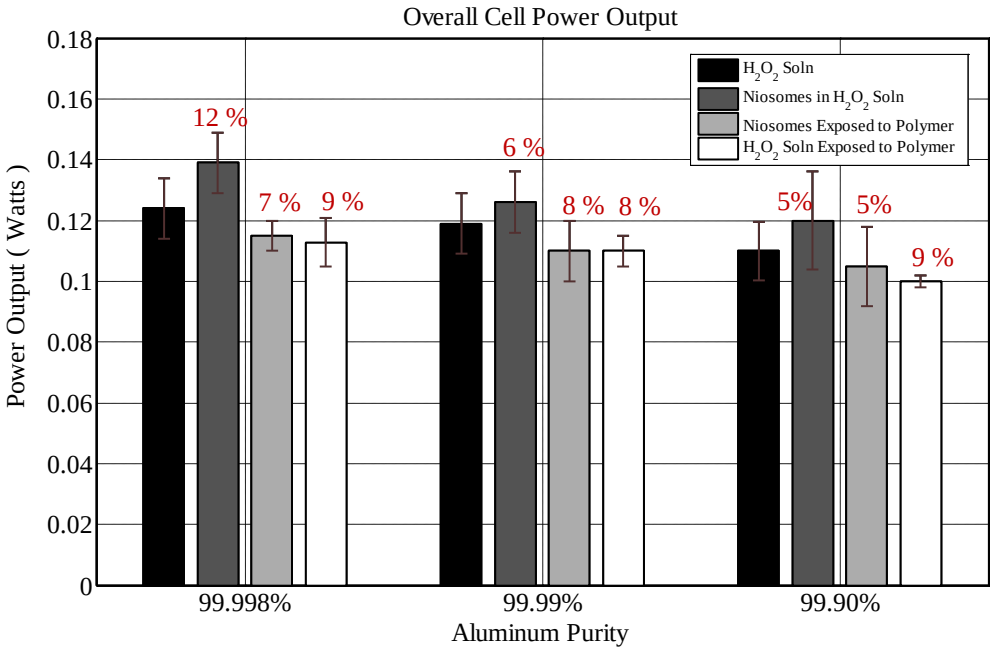

Figure 32: Average Overall Cell Power Output Values for Al Purities: 99.998%, 99.99%, & 99.90% (Numbers in Red Indicated Percent Change Compared to Control)

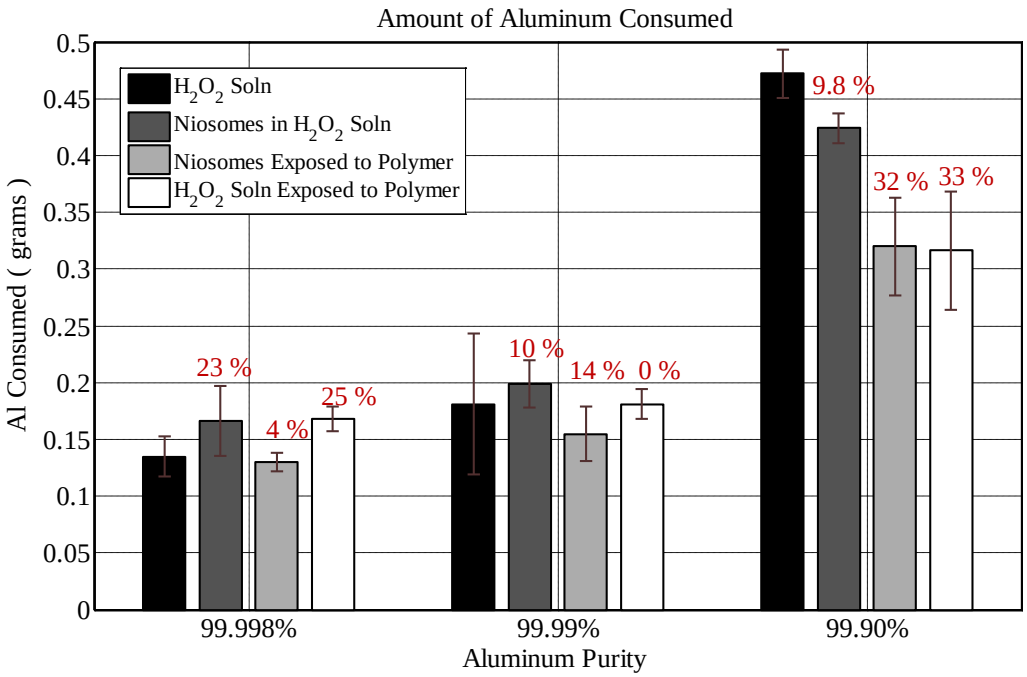

Figure 33: Average Aluminum Consumption Values for Al Purities: 99.998%, 99.99%, & 99.90% (Numbers in Red Indicated Percent Change Compared to Control)

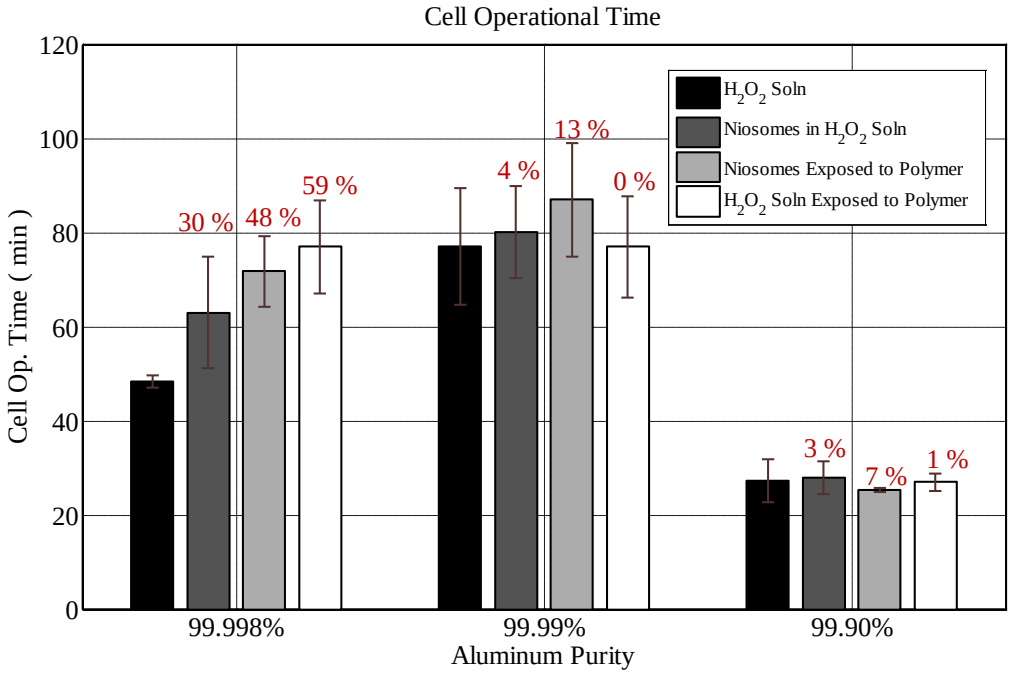

Figure 34: Average Cell Operational Time Values for Al Purities: 99.998%, 99.99%, & 99.90% (Numbers in Red Indicated Percent Change Compared to Control)

Diminishing average overall cell power output values are observed in Figure 32 as aluminum purity decreases. Reviewing numerical values for the different three cases reveals highest average work and cell operational time values for aluminum purity of 99.99%, displayed in Table 5 and Figure 34. As a result of higher cell operational times, cell overall average power output values were below values for aluminum purity of 99.998%.

Table 5: Average Energetic Output for Al Purities: 99.998% & 99.99%

Amount of Work (KJ)	99.998% Al	99.99% Al
H_2O_2 Soln (Control)	0.358 +/- 0.025	0.542 +/- .05
Niosomes in H_2O_2 Soln	0.525 +/- 0.109	0.606 +/- 0.096
Niosomes Exposed to Polymer	0.496 +/- 0.052	0.57 +/- 0.09
H_2O_2 Soln Exposed to Polymer	0.52 +/- 0.067	0.52 +/- 0.047

Average aluminum consumption values display a trend of increasing as aluminum purity decreases for all experimental cases. Among all experimental cases, the use of niosomes in suspension with the polymer resulted in the lowest amount of aluminum consumed for purities 99.998% and 99.99%. Comparing average values between all cases for both purities resulted in less than a 10% difference in values. The average values were significantly highest with the use of 99.90% aluminum purity. Values for aluminum purity of 99.90% were more than 50% higher compared to those for 99.998% and 99.99% aluminum purities. As an outcome to a large consumption of aluminum, values for energy per gram of aluminum where 70% less compared to aluminum purities of

99.99% and 99.998% (Figure 35). In addition, there was a significant decrease of more than two folds in cell operational times as a result of an increase in impurities present in the electrode's material. In both aluminum purities of 99.998% and 99.99%, the novel control reagent release system accomplished highest energy per consumption of aluminum values (4% difference in value seen in Figure 35). Taking into consideration the cost of aluminum purity and the generated average value for energetic output, aluminum purity of 99.90% outperformed the higher purities of aluminum. Average energetic output values divided by dollar amount of aluminum consumed (cost of aluminum purities were $3.33 / gram of Al, $ 2.63 / gram of Al, and $ 0.02 / gram of Al for 99.998%, 99.99%, and 99.90% respectively) ratio values were highest with aluminum purity of 99.90% due to its' low cost (in comparison to the other two purities) as reported in Figure 36. Reviewing ratio values for the two highest aluminum purities reveal aluminum purity of 99.99% achieved greater values for all experimental cases (Figure 37). This is attributed to aluminum purity of 99.99% obtaining higher average energetic output values in comparison to aluminum purity of 99.998%, refer to Table 5.

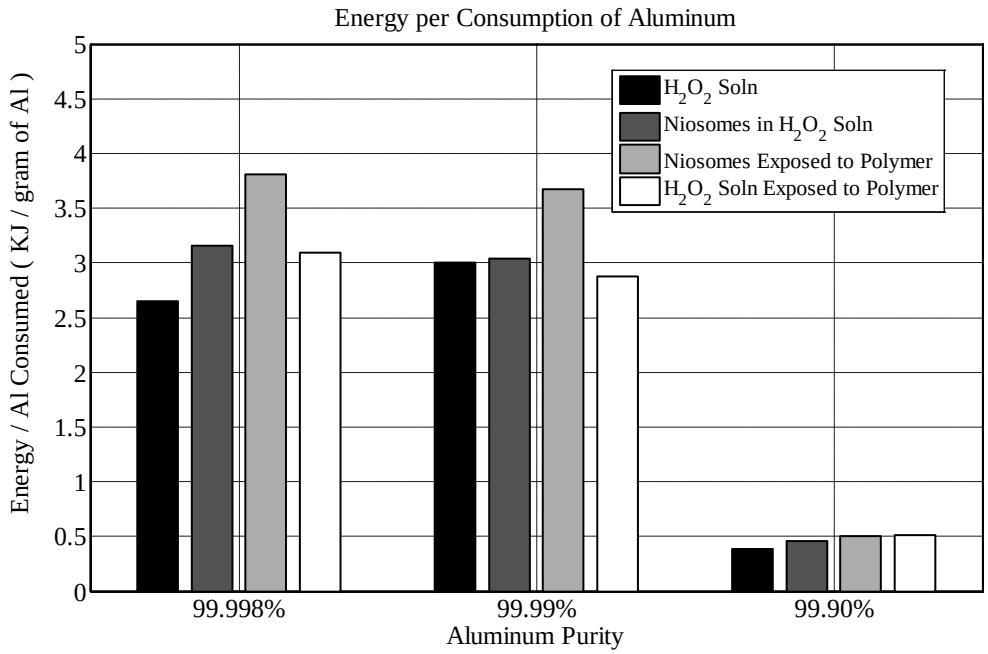

Figure 35: Energy (KJ) per Consumption of Aluminum (gram of Al) for Al Purities: 99.998%, 99.99%, & 99.90%

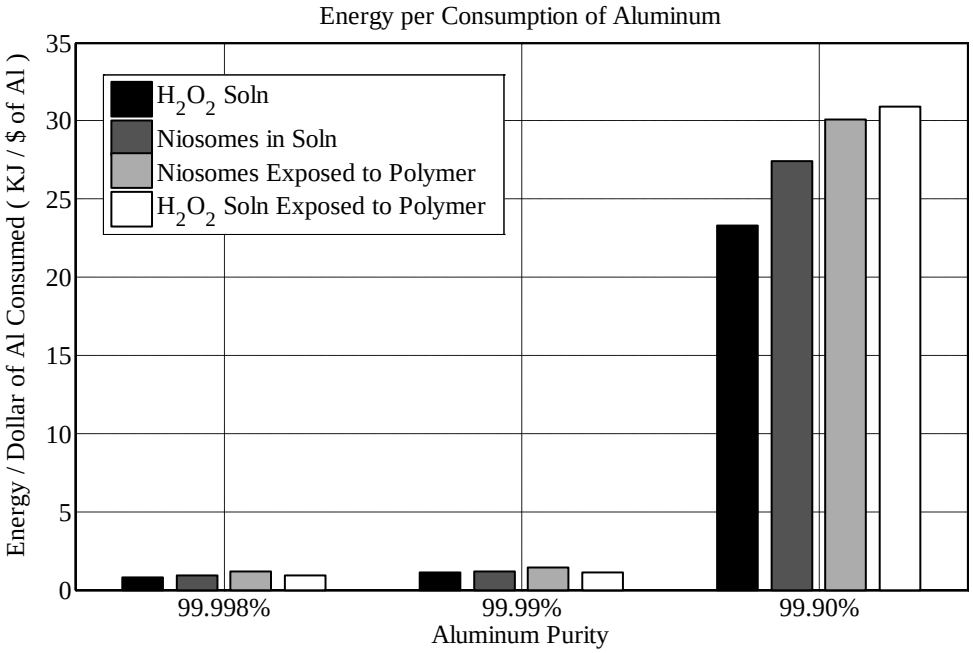

Figure 36: Energy (KJ) per Consumption of Aluminum (Dollar of Al) for Al Purities: 99.998%, 99.99%, & 99.90%

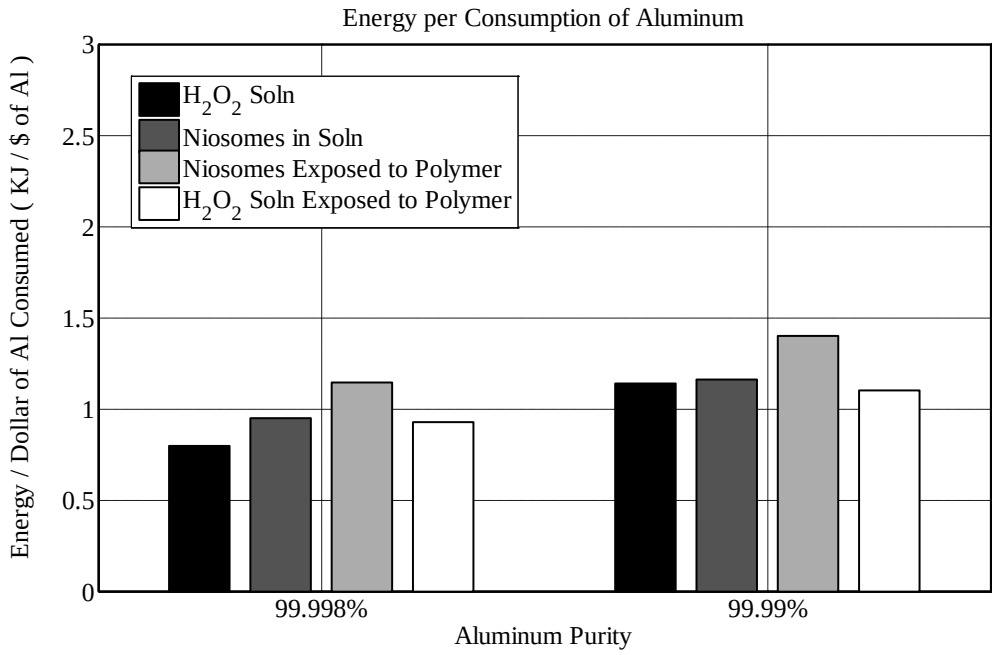

Figure 37: Energy (KJ) per Consumption of Aluminum (Dollar of Al) for Al Purities: 99.998% & 99.99%

4.2.5 Investigation of Proposed System with Alternating the Degree of Cross-linking for Poly(N-isopropylacrylamide) Polymer

The polymer is the second control element over the release of H_2O_2. Results presented thus far have revealed the proposed system advantages over traditional Al / H_2O_2 electrochemical cells with lower average aluminum consumption values and higher obtained average energetic output values. In addition, longer cell operational times and higher energy per gram of aluminum consumed values were achieved. To improve upon the proposed system further, altering the degree of cross-linking for the selected polymer was considered. In the following study, the BisAAm (polymer cross-linker) solution density used in the polymerization process was varied, ranging from 0.005 g of BisAAm per mL of solution to 0.04 g of BisAAm per mL of solution. Heat was applied to solutions greater than 0.02 g of BisAAm per mL of solution to achieve a uniformed mixture. The results from this investigation of varying amounts of BisAAm (cross-linker) for polymers will offer insight into the affects a polymer's degree of crosslinking has once implemented into the proposed system under investigation (in this body of work) on cell characteristics. The cross-linker solution densities utilized and their corresponding mole amounts used during polymer preparation are shown below.

- 0.005 grams of BisAAm / mL of solution – 1.1 µmoles
- 0.01 grams of BisAAm / mL of solution – 2.21 µmoles
- 0.02 grams of BisAAm / mL of solution – 4.41 µmoles
- 0.025 grams of BisAAm / mL of solution – 5.51 µmoles
- 0.04 grams of BisAAm / mL of solution – 8.82 µmoles

There were three replicates conducted to provide an average cell overall power output value for all polymers of different degrees of cross-linking (as well as for other cell characteristics). All experiments were conducted with the use of aluminum purity of 99.99%. The reason as to why this purity was selected is due to its ability to achieve the highest average energetic output values and average cell operational times demonstrated in the 4.2.4. As the BisAAm solution becomes more concentrated, denser polymers will be achieved since there is an increase in the amount of BisAAm present in the polymer (cross-linker). Visa versa as the BisAAm solution decreases, the polymers that will result are less dense appearing less rigid in structure. To better fine tune the proposed system with the use of altering the selected polymer's degree of cross-linking, comparisons to the control where made and percent change values reported for all cell characteristics.

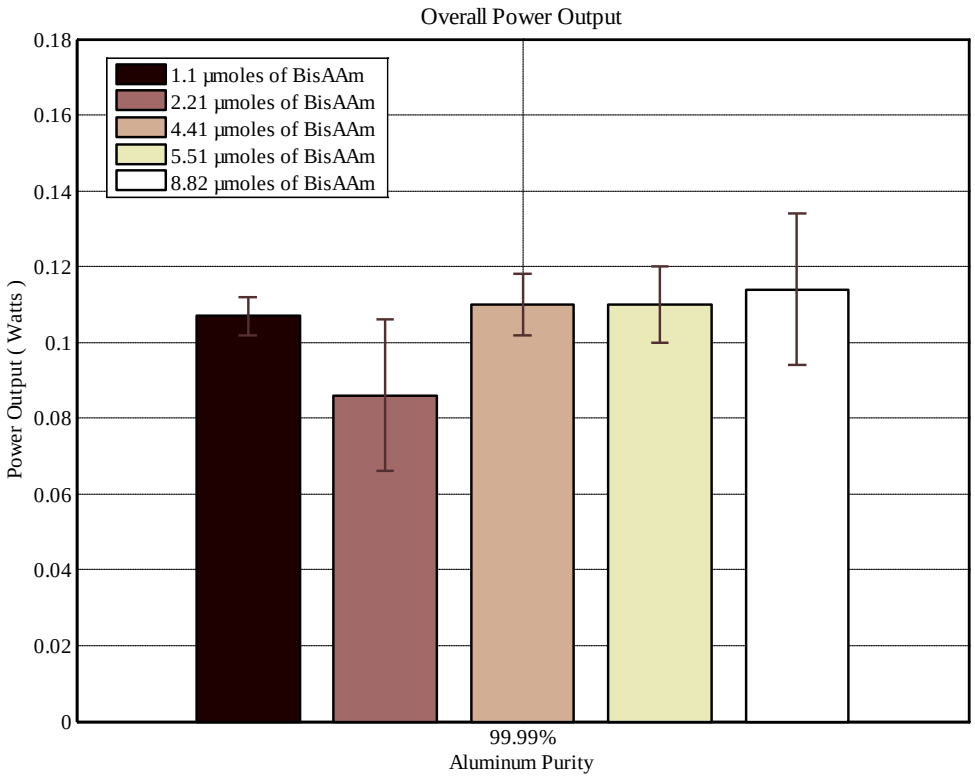

Figure 38: Average Cell Overall Power Output Values Utilizing Al Purity 99.99% with Varying Amounts of BisAAm (Polymer Cross-Linker)

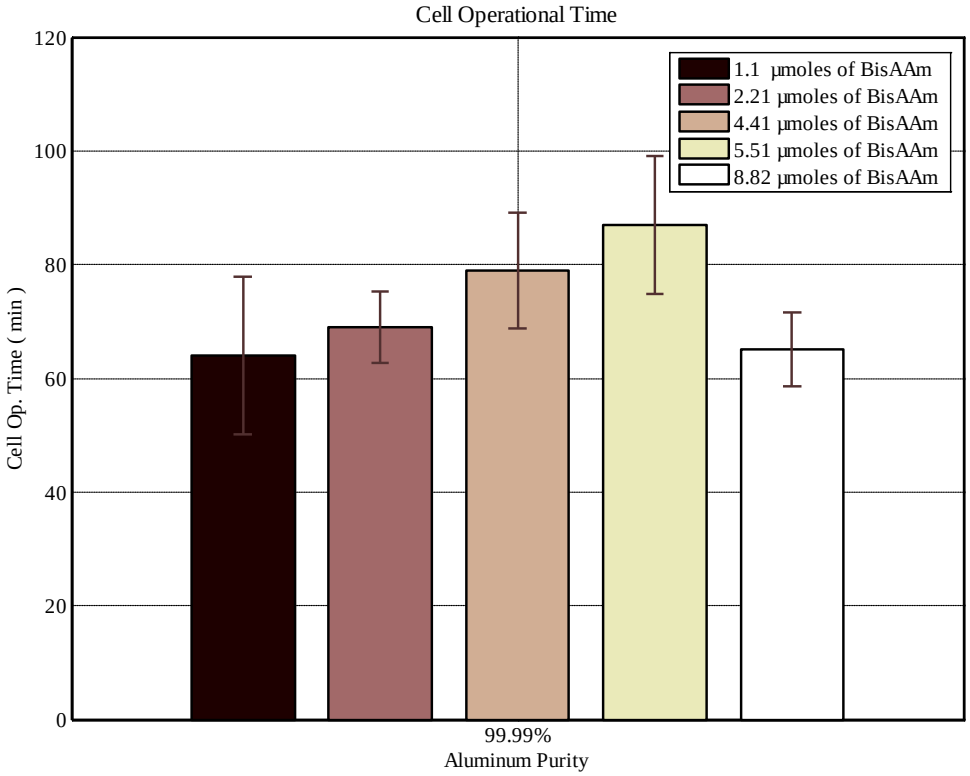

Figure 39: Average Cell Op. Time Values Utilizing Al Purity 99.99% with Varying Amounts of BisAAm (Polymer Cross-Linker)

Average cell overall power output values for each polymer with the presence of niosomes were lower than the control (expected due to results obtained in section 4.2.2). Polymers with 4.41 and 5.51 µmoles of BisAAm achieved higher average energetic output values in comparison to the control (0.56 KJ +/- 0.087 KJ and 0.570 KJ +/- 0.09 KJ respectively). Statistical significance testing (student's t-test) was conducted on experimental energetic output values obtain for 4.41 and 5.51 µmoles of BisAAm against the control experimental values. The null hypothesis is that the two mean values for energy output are the same. A two-sample t-test results in failure to reject the null hypothesis at the 5% significance level in either case. Polymers with 4.41 and 5.51

µmoles of BisAAm delivered higher average cell operational times of 79 min +/- 10.2 min and 87 min +/- 12.1 min (Figure 39). As a result to an increase in cell operational time, average cell overall power output values attained were lower with a value of 0.11 W for both polymers (in comparison to the control, 0.119 W). Polymers with 1.1 and 2.21 µmoles of BisAAm had the lowest values for power output (0.107 W +/- 0.005 W and 0.086 W +/- 0.02 W respectively). The polymer with 8.82 µmoles of BisAAm produced the prominent average power output value among all with a value of 0.114 W (Figure 38). Statistical significance testing (student's t-test) was conducted on experimental power output value obtain 8.82 µmoles of BisAAm against the control's experimental power output value. The null hypothesis is that the two mean values for power output are the same. A two-sample t-test results in failure to reject the null hypothesis at the 5% significance level.

Table 6: Percent Decrease in Power Output Value Compared to Control (0.119 W)

µmoles of BisAAm	Percent Change (%)
1.1	10
2.21	28
4.41	8
5.51	8
8.82	4

Percent change from the control's average value of aluminum consumption (0.181 grams) was calculated for the different polymers with varying amounts of BisAAm. For polymers with amounts of 4.41 µmoles of BisAAm or higher, aluminum consumption values are lower than the control, as reported in Figure 40. This is attributed to the polymers' rigidity in comparison to polymers with amounts of BisAAm below 4.41 µmoles. In addition in Figure 40, aluminum consumption was found to increase with amounts of 1.1 and 2.21 µmoles of BisAAm. Due to previous findings of a decrease in power output values, polymers with 1.1 and 2.21 µmoles of BisAAm are not improving cell efficiency. In contrast, polymers with 4.41 and 5.51 µmoles of BisAAm have achieved higher average amounts of work, longer cell operational times, and consume lower quantities of aluminum. Results in addition indicate that there is a maximum amount of cross-linker optimal for improving upon cell characteristics and that value is 5.51 µmoles of BisAAm. Increasing the degree of cross-linking above 5.51 µmoles of BisAAm will prevent encapsulated niosomes from diffusing into the polymer (the second control element over the cathodic reactant H_2O_2).

Table 7: Percent Change in Al Consumption Value Compared to Control (0.181 g Al): Red Value Indicate an Increase in Al Consumption

µmoles of BisAAm	Percent Change (%)
1.1	12
2.21	17
4.41	21
5.51	15
8.82	12

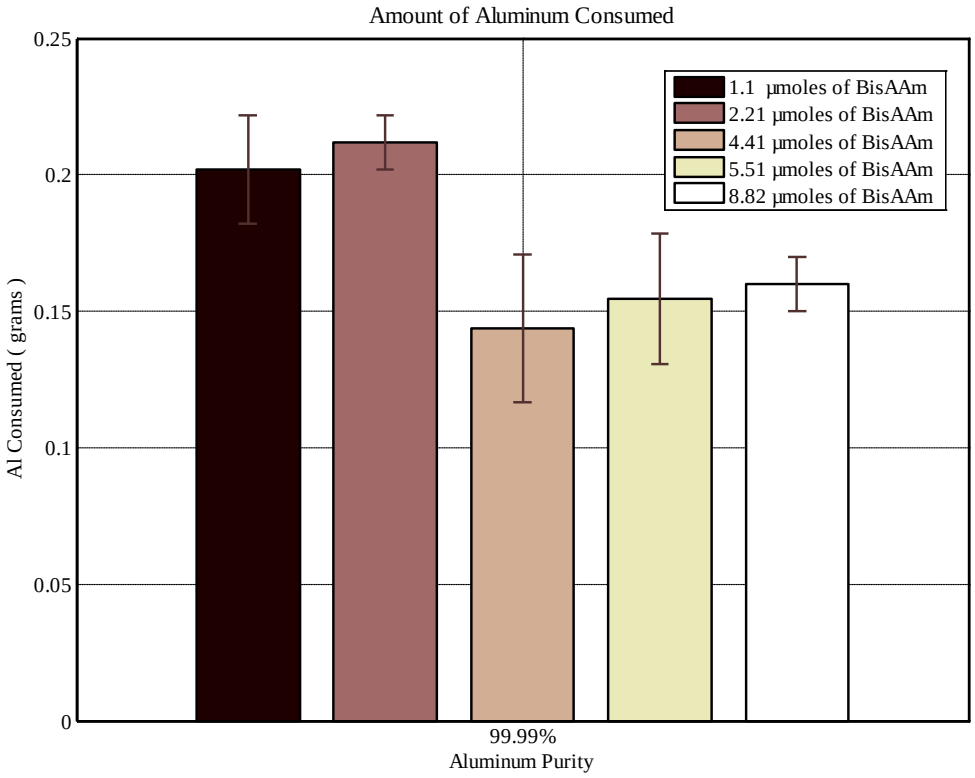

Figure 40: Al Consumption Average Values Utilizing Al Purity 99.99% with Varying Amounts of BisAAm (Polymer Cross-Linker)

Due to lower quantities of aluminum consumption and higher energetic outputs, polymers with 4.41 and 5.51 41 µmoles of BisAAm (polymer cross-linker) achieved higher energy per grams or dollars of aluminum consumed values in comparison to the control (31% and 22% increase respectively) as reported in Table 8. The control's energy per grams of aluminum consumed resulted to be approximately 3 (Figures 26). The

investigation of the effects a polymer's rigidity has once implemented into the proposed system reveals that polymers with less than 4.41 µmoles of BisAAm are unsuitable. In addition, the use of 4.41 and 5.5 µmoles of BisAAm in polymers are optimal for the proposed system. The implementation of these polymers in the novel proposed system supports the aim of lowering aluminum consumption for material conservation that will in return prolong the utilization of the electrochemical cell.

Table 8: Average Energetic Output Obtained / Average Value of Al Consumed; Values Utilizing Al Purity 99.99% with Varying Amounts of BisAAm (Polymer Cross-Linker)

Work / Al Consumed :	KJ / g of Al	KJ / $ of Al
1.10 µmoles of BisAAm	2.06	0.147
2.21 µmoles of BisAAm	1.67	0.119
4.41 µmoles of BisAAm	3.93	0.28
5.51 µmoles of BisAAm	3.67	0.262
8.82 µmoles of BisAAm	2.77	0.198

Chapter 5: Conclusion and Future Work

5.1 Summary of Findings

Results obtained by the DLS apparatus indicate that a uniform size distribution is not achieved after the niosomes have been extruded. In addition, the size distribution for each of the three batches tested is inconsistent with each other. Niosome's hydrodynamic diameter for three batches was monitored with time. Results indicate the niosomes in each different batch to be instable (due to the niosomes rupturing and reforming into different sized vesicles as time increases). Although Figure 20 suggest that the niosomes converge to a similar size after 9 days, further testing is required. In addition, further investigation is required to properly assess size distribution before and after extrusion that would incorporate additional niosome batches, measurement taken before sonication, and altering pore size for membrane used during extrusion. Future work might indicate that the sonication of niosomes might suffice and ultimately save future users time and money.

The investigation of the proposed system, utilizing aluminum purity 99.99%, demonstrated that the introduction of niosomes in suspension resulted in the highest increase of average cell overall power output value compared to the control (with a 6 % increase). Even though average power output values were lower, the average amount of energetic output value obtained with the novel proposed system was higher than the control and additionally average cell operational time increased by 13%. The presence of

niosomes in the proposed system increases the average amount of work obtained versus the use of the polymer without niosomes justifying the need of niosomes. There was a decrease of 15% in average aluminum consumption value with the proposed novel system (niosomes exposed to the polymer). Results confirm that the presence of niosomes is attributed to the decrease in aluminum consumption due to higher values with the use of a polymer without the presence of niosomes in the Al / H_2O_2 electrochemical cell (experimental case 4). Utilizing the proposed system (suspended niosomes exposed to the polymer) resulted in an increase in energy per gram of aluminum consumed due to the 15% decrease in average aluminum consumption value (compared to the control). In conclusion, the proposed system supports the aim of lowering aluminum consumption for material conservation that will in return prolong the utilization of the cell.

The investigation conducted to determine the effects SPAN 40 versus SPAN 60 would have on the systems in this study concluded that the use of SPAN 60 niosomes in suspension outperformed SPAN 40 niosomes in average cell overall power output with a 14% difference in value.

The use of SPAN 40 niosomes in suspension consumed less aluminum compared to niosomes composed of SPAN 60 surfactant in suspension. The difference in average aluminum consumption values was expected due to the higher average amount of work obtained from the use of SPAN 60 niosomes versus SPAN 40 niosomes. The percent difference between both aluminum consumption average values is approximately 12%. In the utilization of the proposed system, the percent difference between average aluminum consumption values was 7%. Although similar average cell operational time and discrete

average work values were observed, SPAN 60 niosomes were successful in reducing parasitic reactions due to the difference in aluminum consumption.

Investigating the influence of aluminum purity upon the comparison between the control to competing systems demonstrated that average cell overall power output values were highest amongst all experimental cases and aluminum purities for the use of niosomes in suspension (without exposure to a polymer). This is attributed to the niosomes achieving higher average work values compared to the control, the proposed system, and the use of the polymer without niosomes present. Percent change values, in comparison between the control to all three cases, were highest for aluminum purity of 99.998% when reviewing average energetic output values and average cell operational times. Diminishing average overall cell power output values are observed as aluminum purity decreases.

Average aluminum consumption values displayed a trend of increasing as aluminum purity decreased for all experimental cases. The use of niosomes in suspension with the polymer resulted in the lowest average amount of aluminum consumed for purities 99.998% and 99.99%. As a result, both aluminum purities of 99.998% and 99.99% accomplished highest energy per consumption of aluminum values (small 2% difference in value between the proposed system with different purities).The values for aluminum consumption were significantly highest with the use of 99.90% aluminum purity.

Average energetic output values divided by dollar amount of aluminum consumed (cost of aluminum purities were $3.33 / gram of Al, $ 2.63 / gram of Al, and $ 0.02 /

gram of Al for 99.998%, 99.99%, 99.90% respectively) ratio values were highest with aluminum purity of 99.90% due to its' low cost (in comparison to the other two purities). Reviewing ratio values for the two highest aluminum purities reveal aluminum purity of 99.99% achieved greater values for all experimental cases. This is attributed to aluminum purity of 99.99% obtaining higher average energetic output values in comparison to aluminum purity of 99.998%.

To improve upon the proposed system further, BisAAm amounts (polymer cross-linker) were varied to alter the polymer's degree of cross-linking. Results reveal that polymers with less than 4.41 µmoles of BisAAm are unsuitable. In addition, the use of 4.41 and 5.5 µmoles of BisAAm in polymers are optimal for the proposed system. The implementation of these polymers in the novel proposed system supports the aim of lowering aluminum consumption for material conservation that will in return prolong the utilization of the cell. Results in addition indicate that there is a maximum amount of cross-linker optimal for improving upon cell characteristics and that value is 5.51 µmoles of BisAAm. Increasing the degree of cross-linking above 5.51 µmoles of BisAAm will prevent encapsulated niosomes from diffusing into the polymer (the second control element over the cathodic reactant H_2O_2).

5.2 Future Work Recommendations

5.2.1 Continuing Niosome Size Characterization

Further investigation is required to properly assess size distribution before and after extrusion that would incorporate additional niosome batches, measurement taken before sonication, and altering pore size for membrane used during extrusion. Future work might indicate that the sonication of niosomes might suffice and ultimately save future users time and money. In addition, alteration to cholesterol and DCP amounts for the formation of SPAN 40 niosomes could possibly result in smaller size distributions.

5.2.2 Future Cell Potential Experiments

Future work to further the investigation on providing control over the release of the cathodic reagent, in order to reduce parasitic reactions, includes testing the proposed system under a range of loads as well as a range of different weight percentage of H_2O_2 solutions. In addition, monitoring temperature during experimental runs would provide helpful insight upon the amount of energy exerted during each run. In literature, it has been speculated that increasing anode surface area in combination with a small cell volume would allow the use of lower H_2O_2 concentration and result in higher electrochemical reaction efficiencies [10]. Exploring the use of a granular aluminum anode [22] with the proposed system may increase cell efficiency and allow the use of lower H_2O_2 concentration.

Furthermore, determining the concentration of niosomes present in each experimental run is a valuable piece of information worth perusing and acquiring for future cell potential experiments. Different concentration amounts of niosomes may have

an effect on experimental runs conducted (involving their use). In addition, if the niosomes were to be embedded into the polymer's matrix this could potentially offer a significant increase over the control of the oxidizing reagent.

5.3 Final Remarks

In summary, results have revealed the proposed system advantages over the traditional Al/ H_2O_2 electrochemical cell with lower average aluminum consumption values and higher obtained average energetic outputs. In addition, longer cell operational times and higher energy per gram or dollar of aluminum values were achieved. Due to the achievement of longer cell operational times, the implementation of the proposed system resulted in lower cell overall average power output values. In contrary, the utilization of niosomes in suspension without the polymer did accomplish a higher average power output in comparison to the traditional Al / H_2O_2 electrochemical cell.

References

1. Linden, D., *Handbook of Batteries*. 2 ed, ed. D. Linden. 1995: McGraw-Hill Illustrated. 1216.

2. Carl H. Hamann, A.H., Wolf Vielstich, *Electrochemistry* 2nd ed. 2007: Chapman & Hall. 550.

3. Colin A. Vincent, B.S., *Modern Batteries: An Introduction to Electrochemical Power Sources*. 2nd ed. 1997: Butterworth-Heinemann. 351

4. Nie Luo, G.H.M., Richard Gimlin, Rodney Burton, *Hydrogen-peroxide-based fuel cells for space power systems* Journal of Propulsion and Power, 2008. 24(3): p. 583-589.

5. Oistein Hasvold, K.H.J., Ole Mollestad, Sissel Forseth, Nils Storkersen, *The alkaline aluminum/hydrogen peroxide power source in the Hugin II unmanned underwater vehicle.* Journal of Power Sources, 1999. 80: p. 254-260.

6. Commission, C.E. *Fuel Cell Vehicles*. 2012 [cited 2012 3-25-12]; Available from: http://www.consumerenergycenter.org/contactus.html.

7. Scibioh, B.V.a.M.A., *Fuel Cells Principles and Applications*. 2007, Hyderabad Universities Press (India) Private Limited

8. *The Primary Battery* ed. G.W.H.a.N.C. Cahoon. Vol. 1. 1971: John Wiley & Sons, INC. 500.

9. A M Cardenas-Valencia, J.D., J Bumgarner, L Langebrake, W Moreno *Long shelf-life, Al-anode micro-fabricated cells activated with alkaline-H2O2 electrolytes.* Journal of Micromechanics and Microenegineering, 2006. 16: p. 1511-1518.

10. Russell R. Bessette, M.G.M., Charles J. Patrissi, Craig M. Deschenes, Christopher N. LaFratta, *Development and characterization of a novel carbon fiber based cathode for semi-fuel cell applications.* Journal of Power Sources, 2001. 96: p. 240-244.

11. David J. brodrecht, J.J.R., *Aluminum-hydrogen peroxide fuel-cell studies.* Applied Energy, 2003. 74: p. 113-124.

12. Robert Frederick Benson, A.M.C.-V., Lawrence C. Langebrake, *Aluminum and Solid Alkali Peroxide Galvanic Cell* 2010, University of South Florida: United States of America.

13. Qingfeng Li, N.J.B., *Aluminum as anode for energy storage and conversion: a review*. Journal of Power Sources, 2001. 110 p. 1-10.

14. Andres M. Cardenas-Valencia, R.T.S., Lori R. Adornato, Larry C. Langebrake, *Recent development of semi-fuel cells for powering underwater sensors and platforms.* ECS Transactions 2012. 26(1): p. 417-429.

15. U.S. Peroxide, L. *Standard Electrode Potentials* 2012 [cited 2012 3-25-12]; Available from: http://www.h2o2.com/technical-library/physical-chemical-properties/thermodynamic-properties/default.aspx?pid=50&name=Standard-Electrode-Potentials.

16. Licht, S., *Novel aluminum batteries: a step towards derivation of superbatteries.* Colloids and Surfaces A: Physicochemical and Engineering Aspects 1998. 134: p. 241-248.

17. Russell R. Bessette, J.M.C., Dwayne W. Dischert, Eric G. Dow, *A study of cathode catalysis for the aluminum/hydrogen peroxide semi-fuel cell.* Journal of Power Sources, 1999. 80: p. 248-253.

18. A.M. Cardenas-Valencia, J.D., S. Knighton, C.J. Biver, J. Bumgarner, L. Langebrake, *Aluminum-anode silicon-based micro-cells for powering expendable MEMS and lab-on-a-chip devices.* Senors and Actuators B 2007. 122: p. 328-336.

19. Eric G. Dow, R.R.B., G.L Seeback, C. Marsh-Orndorff, H. Meunier, J. VanZee, M.G. Medeiros, *Enhanced electrochemical performance in the development of the aluminum/hydrogen peroxide semi-fuel cell.* Journal of Power Sources, 1997. 65: p. 207-212.

20. J. M. Wang, J.B.W., H.B. Shao, X.X. Zeng, J.Q. Zhang, C.N. Cao, *Corrosion and electrochemical behaviors of pure aluminum in novel KOH-ionic liquid-water solutions.* Materials and Corrosion, 2009. 60: p. 977-981.

21. A.M. Abdel-Gaber, E.K., H. Abo-Eldahab, Sh. Adeel, *Novel package for inhibition of aluminum corrosion in alkaline solutions.* Materials Chemistry and Physics, 2010. 124: p. 773-779.

22. Neil A. Popovich, R.G., *Studies of granular aluminum anode in an alkaline fuel cell* Journal of Power Sources, 2002. 112: p. 36-40.

23. Weiqian Yang, S.Y., Wei Sun, Gongquan Sun, Qin Xin, *Nanostructured silver catalyzed nickel foam cathode for an aluminum-hydrogen peroxide fuel cell.* Journal of Power Sources, 2006. 160: p. 1420-1424.

24. A. M. Cardenas-Valencia, D.F., H. Broadbent, L. Langebrake, R. F. Benson *Micro-actuated aluminum galvanic and semi-fuel cells for powering remote lab on a chip applications* in *The 7th International Conference on Miniaturized Cheimcal and Biochemical Analysis Systems* 2003.

25. Cardenas-Valencia, A., *Method of control delivery for use of electrochemical power source*. 2011: USA.

26. Ijeoma F. Uchegbu, S.P.V., *Non-ionic surfactant based vesicles (niosomes) in drug delivery*. International Journal of Pharmaceutics 1998. 172: p. 33-70.

27. Ijeoma F. Uchegbu, A.T.F., *Non-ionic Surfactant Vesicles (Niosomes): Physical and Pharmaceutical Chemistry*. Advance in Colloid and Interface Science 1995. 58: p. 1-55.

28. Dearborn, K.O.-H., *The Characterization of Non-Ionic Surfactant Vesicles: A Release Rate Study for Drug*, in *Department of Chemical and Biomedical Engineering*. 2006, University of South Florida: Tampa. p. 225.

29. Fahima Hashim, M.E.-R., Mohamed Nasr, Yasmin Abdallah, *Preparation and characterization of niosomes containing ribavirin for liver targeting* Drug Delivery, 2010. 17: p. 282-287.

30. Selim Kara, O.P., *Phase transitions of N-isopropylacrylamide gels prepared with various crosslinker contents.* Materials Chemistry and Physics, 2003. 80: p. 555-559.

31. Cates, R.S., *Influence of Crosslink Density on Swelling and Conformation of Surface-Constrained Poly(N-Isopropylacrylamide) Hydrogels*, in *Department of Chemical and Biomedical Engineering*. 2010, University of South Florida: Tampa. p. 95.

32. R. Salgado-Rodriguez, A.L.-C., K.F. Arndt, *Random copolymers of N-isopropylacrylamide and methacrylic acid monomers with hydrophobic spacers: PH-tunable temperature sensitive materials.* European Polymer Journal, 2004. 40: p. 1931-1946.

33. Roberto F.S. Freitas, E.L.C., *Temperature sensitive gels as extraction solvents.* Chemical Engineering Science, 1987. 42(1): p. 97–103.

34. Ebrahim Vasheghani-Farahani, D.G.C., Juan H. Vera, Martin E. Weber, *Concentration of large biomolecules with hydrogels.* Chemical Engineering Science, 1992. 47(1): p. 31–40.

35. Karl-Friedrich Arndt, D.K., Andreas Richter, *Application of sensitive hydrogels in flow control.* Polymers for Advanced Technologies, 2000. 11(8-12): p. 496-505.

36. Teruo Okano, A.K., Yasuhisa Sakuraia, Yoshiyuki Takeib, Naoya Ogatab, *Temperature-responsive poly(N-isopropylacrylamide) as a modulator for alteration of hydrophilic/hydrophobic surface properties to control activation/inactivation of platelets.* Journal of Controlled Release, 1995. 36(1-2): p. 125–133.

37. Toshimitsu Yoshioka, B.S., Alexander T. Florence, *Preparation and properties of vesicles (niosomes) of sorbitan monoesters (Span 20, 40, 60, and 80) and a sorbitan triester (Span 85).* International Journal of Pharmaceutics, 1994. 105: p. 1-6.

38. Lipids, A.P., *Cholesterol Figure*, in *Avanti Polar Lipids Database*. 2012.

39. Biomedicals, M., *Dicetyl Phosphate Free Acid Figure*, in *MP Biomedicals Database*. 2012.

40. Sigma-Aldrich, *N-Isopropylacrylamide Figure*, in *Sigma-Aldrich Database*. 2012, Sigma-Aldrich Co. .

41. Sigma-Aldrich, *N,N'-Methylenebis(acrylamide) Figure*, in *Sigma-Aldrich Database*. 2012.

42. Andres M. Cardenas-Valencia, S.O., Larry C. Langebrake, R. Timothy Short, *Aluminum-alkali peroxide cells for "in-the-field" power sources development* Applied Energy, 2012.

43. Chu, B., *Laser light scattering: basic principles and practice*. 1991, Boston: Academic Press.